Phosphatidylcholine Metabolism and ACAT Affect the Trafficking of LDL-derived Free Cholesterol in Cholesterol-loaded CHO Cells

CHANDRA LANDRY

Thesis submitted to the Faculty of Graduate and Postdoctoral Studies

In partial fulfillment of the requirements

For the degree of

MASTER of SCIENCE

Department of Biochemistry, Microbiology and Immunology

University of Ottawa

Ottawa, Ontario, Canada

Abstract

In vitro studies have shown that the major membrane phospholipid phosphatidylcholine (PC) can positively influence the incorporation of cholesterol in lipid membranes. The influence of PC on the cellular trafficking of LDL-derived free cholesterol was investigated. Sterol regulatory-defective (SRD)-4 cells are Chinese hamster ovary (CHO)-derived fibroblasts that display vastly elevated rates for the synthesis and catabolism of PC. SRD-4 cells harbor two known gene mutations: a mutation in the functional allele for SCAP, resulting in defective feedback suppression of cholesterol biosynthesis; and a loss-of-function mutation in the functional allele for acyl-CoA:cholesterol acyl transferase (ACAT), an endoplasmic reticulum (ER)-localized enzyme that esterifies free cholesterol. Incubation of SRD-4 cells with 50 μg/ml low density lipoprotein (LDL) for 18 h resulted in lysosomal accumulation of free cholesterol as revealed by filipin staining. This accumulation was not evident following LDL treatment of parental CHO7 cells, and was blunted in SRD-2 cells that express a constitutively-active form of SREBP-2 and overproduce cholesterol but have functional ACAT activity. Treatment of SRD-2 cells with LDL in the presence of an ACAT inhibitor 58-035 resulted in robust lysosomal cholesterol accumulation that was reversible upon drug washout, supporting that cholesterol trafficking in cholesterol-loaded cells is dependent on ACAT activity and, more specifically, ER free cholesterol levels. Lysosomal accumulation of LDL-derived cholesterol was prevented in SRD-4 cells supplemented with lyso-PC (50 μM), a substrate for PC synthesis through the reacylation pathway, and also in cells treated with bromoenol lactone (BEL), an inhibitor of phospholipase A2 implicated in bulk PC turnover. In a counter study, lysosomal LDL-derived cholesterol accumulation was induced in parental CHO-7 cells using R-propranolol, which inhibits the conversion of phosphatidic acid to diacylglycerol (DAG), a substrate in the CDP-choline pathway. This blockage was also relieved through co-treatment with lyso-PC. These studies support that PC to free cholesterol ratios in downstream organellar membranes can influence cholesterol trafficking out of lysosomal compartments in cholesterol-loaded cells.

This Thesis is dedicated to my Parents,
The most hardworking and selfless people I know

‘It’s never too late to be who you might have been.’
George Eliot

Acknowledgments

The list of people that have helped me with this work seems endless, as I have been lucky enough to have constant support and guidance from all areas of my life. First and foremost, I would like to thank my supervisor, Thomas Lagace. His direction and patience were indispensible, but it was mainly his ability to remind me that a failed experiment is not the end of the world that I needed most (and most often). Also, I would like to thank those who have been involved on my thesis committee over the years: Drs. Yves Marcel and Xiaohui Zha.

I am forever grateful to have worked with the people of the Heart Institute; especially those on the 4th floor. It would have been a much different journey otherwise. They were always available for help with optimization, finding a hidden chemical, fixing a hopelessly broken piece of equipment or just letting me talk when I needed it most (which is what happened in most cases). Anna Toma was especially helpful when I wound myself up about something that I was sure was going to doom my project; her patience was limitless. I have made countless friendships during my time at the Heart Institute, and I have grown more than I ever thought possible in such a short amount of time. I owe that to everyone who has encouraged me during these past few years.

I cannot express enough thanks to my friends; I can honestly say that my sanity would not be intact if not for my amazing friends Heather Sarazin and Geoffrey Leblond. Oddly enough, my liver might be more intact if not for them.

My parents may not understand what I do in the lab, but they were always encouraging and willing to let me 'borrow' groceries and anything else I needed without comment.

Finally, I would like to thank my wonderful boyfriend, Bryan Lefebvre. He came into my life in the middle of this degree, and was not only brave enough to stick around, but managed to change my life forever. Whether it was relentlessly listening to me talk about my latest lab related dilemma, or his unwavering ability to make me laugh no matter what situation arose, he was hands down the most amazing thing that could have ever happened to me. I cannot imagine doing this without him by my side, and I'm forever thankful that I didn't have to.

Contents

List of Abbreviations

25-HC	25-Hydroxycholesterol
ABCA1	ATP-binding cassette transporter
ACAT	Acyl-CoA;cholesterol acyl transferase
ACATi	ACAT inhibitor (58-035)
apoA	Apolipoprotein A
apoB	Apolipoprotein B
ATP	Adenosine triphosphate
bp	Base pair
bHLH	Basic helix-loop-helix
BEL	Bromoenol lactone
CCT α	CTP:phosphochilone cytidylyltransferase α
CD	Methyl β-cyclodextrin
CDP-choline	cytidine diphosphate-choline
CHO	Chinese Hamster Ovary Cells
Co-IP	Co-precipitation
CTP	Cytosine triphosphate
Cyclodextrin	Hydroxypropyl-β-cyclodextrin
DAG	Diacylglycerol
EDTA	Ethylenediaminetetraacetic acid
ER	Endoplasmic reticulum
FH	Familial hypercholesterolemia
IDL	Intermediate-density lipoprotein
GPC	Glycerophosphorylcholine
GTPase	Guanosine triphosphate hydrolase
HDL	High-density lipoprotein
HMG-CoA	3-hydroxy-3methylglutaryl-coenzyme A
Insig-1	Insulin-induced genes-1
$iPLA_2$	Calcium-independent phospholipase A2
LAL	Lysosomal acid lipase

LDL	Low-density lipoprotein
LDLR	Low-density lipoprotein receptor
LPDS	Lipoprotein deficient serum
Lyso-PC	L-α-Lysophosphatidycholine
LXR	Liver X receptor
NPC1	Niemman Pick Type C Protein 1
NPC2	Niemman Pick Type C Protein 2
Ox-LDL	Oxidized-LDL
PA	Phosphatidic acid
PAP	Phosphatidic acid phosphatase
PC	Phosphatidylcholine
PE	Phosphatidylethanolamine
PEMT	Phosphatidylethanolamine *N*-methyltrasnferase
Prop	R-Propranolol
S1P	Site-1 protease
S2P	Site-2 protease
SCAP	SREBP cleavage-activating protein
SRD	Sterol regulatory defective cells
SRE	Sterol regulatory element
SREBP	Sterol regulatory binding protein
TG	Triacylglycerides
VLDL	Very low-density lipoprotein

List of Figures

1.1 The Importance of Cholesterol Regulation

The mechanisms of cholesterol regulation have been a highly researched topic, with upwards of 13 Nobel Prizes being awarded for work in the field since 1928 (15). Cholesterol homeostasis is a tightly regulated and controlled process due to its many essential roles within the cell. For example, it helps control membrane fluidity within the cellular membrane and is also used as a precursor for many sterols. A more complete pathway of cholesterol regulation is key to aiding in the treatment of such prominent diseases as familial hypercholesterolemia (FH) and atherosclerosis (17). These can be defined as an increase in the circulating cholesterol content in the plasma and a formation of atherosclerotic plaque within arterial walls, respectively. The precursor to an atherosclerotic plaque is the foam cell. This is formed when there is a dysfunction of the underlying endothelial cells of the artery, and there is an ensuing macrophage and cytokine response. If the low-density lipoprotein (LDL) entering the artery wall are not adequately removed they will become modified from their native state. This generally occurs by the action of free radicals (61). Modified lipids, including oxidized-LDL (ox-LDL), are not under the same control as native LDL, and thus has the ability to enter the macrophage and engorge it with lipids (53). These macrophage foam cells continue to promote lipoprotein retention and monocyte recruitment by secreting proteoglycans and inflammatory cytokines. As this action persists a plaque can progress to a size where the arterial lumen is occluded and the function of the artery can be compromised. In addition, plaque rupture can lead to thrombus formation, triggering a heart attack or stroke. Finding mechanisms to minimize arterial plaque accumulation is of profound interest, due to the high incidence rate of atherosclerosis in the western world (30). These diseases showcase some of the various phenotypes that can

arise due to the dysregulation of cholesterol homeostasis, and further highlight its importance (41).

Cholesterol was first discovered in 1794 and has since been highly characterized. It can be obtained through diet via the absorption of lipids in the epithelial cells of the intestines, followed by packaging into chylomicrons. These particles will then deliver lipids to necessary locations within the body. Cholesterol can also be synthesized in the liver though a multi-step process requiring more than 30 enzymes, starting from the 2 carbon precursor acetate (8, 44). The final cholesterol structure contains 27 carbons and, for the most part, is a non-polar molecule; the exception is a polar hydroxyl group at the carbon-3 position. Due to its unique properties the cholesterol molecule has essential roles in cell membranes, however at elevated concentrations has the potential to be highly cytotoxic. Therefore, the cell has developed mechanisms for highly regulated cholesterol transport, uptake, and synthesis. Improper regulation of these various pathways can cause numerous complications, such as those examples mentioned above.

1.2 Lipoproteins and LDL uptake

1.2.1 Lipoproteins

Apolipoproteins can be insoluble and/or non-exchangeable proteins in nature; they are needed to form and transport lipoproteins. The main function of lipoproteins is to safely and efficiently transport lipids throughout the body. The five major classes of lipoproteins can be broken down into chylomicrons, very low-density lipoprotein (VLDL), intermediate-density lipoprotein (IDL), LDL and high-density lipoprotein (HDL) (5, 19). These structures are characterized by having a monolayer of phospholipids and unesterified

cholesterol as the membrane, with varying densities of cholesteryl esters, free cholesterol and triacylglycerides (TG) within the hydrophobic core. Simply put, a cholesteryl ester is a cholesterol molecule that has had its hydroxyl group esterified to facilitate storage and transportation within the cell. In general, specific apolipoproteins are associated with specific classes of lipoproteins. For example, apolipoproteinB100 (apoB100) is specific to VLDL and LDL, while apoA1 is specific to chylomicrons and HDL (22). Lipoproteins then travel to the liver where the sterols, phospholipids and fatty acids are liberated for use in cell metabolism. The exception is HDL, which functions in the egress of cholesterol from the peripheral tissues to the liver, where it is processed for excretion from the body as bile. This process is known as reverse cholesterol transport (67).

1.2.2 LDL Uptake

A major player in cholesterol regulation is the LDL-receptor (LDLR), which came to light due to the discovery of *LDLR* mutations that decrease receptor function in the progression of FH (18, 41). This receptor is located on the cell surface and can bind to LDL and carry it into the cell via endocytosis in clathrin coated vesicles (40). These vesicles merge with early endosomes, where LDLR undergoes a pH-dependent conformational change, releasing the LDL particle, after which the LDLR recycles back to the cell surface (6). The LDL particle traffics to late endosomes, which mature into lysosomes. This maturation can be accounted for by a decrease in the pH, rendering the lysosome more acidic than its predecessor. This acidic compartment allows optimal conditions for cholesteryl esters packaged in LDL to be degraded via the enzyme lysosomal acid lipase

(LAL), allowing the free cholesterol molecules to be released (**Figure 1.1**). Defects in LAL can lead to cholesterol storage disorder diseases, such as Wolman disease (31).

1.3 The Niemann-Pick type C Proteins

1.3.1 Niemann-Pick type C (NPC) 1 and 2 Proteins

Cholesterol trafficking within the cell is highly dependent on two cholesterol-binding proteins, Niemann-Pick type C (NPC) 1 and NPC2, which allow free cholesterol to move from within the lysosomes to other organelles such as the ER and plasma membrane. Both proteins are located in the lysosomal compartment of the cell. Their mechanism of action has recently come to light; much of this research was accomplished due to Niemann-Pick Type C disease. This disease occurs when inactivating mutations in one of these two proteins arises, thereby causing a failure in the egress of LDL-derived cholesterol from the lysosomal compartments (64). This results in a characteristic punctate lysosomal blockage in the cell that can be viewed with filipin staining, which is specific to unesterified cholesterol. Both proteins have been shown to cause identical disease phenotypes. NPC1 is a large membrane-bound protein located within the membranes of endosomes and lysosomes (21, 28). Contrastingly, NPC2 is a small soluble protein that resides within endosomes and lysosomes, and has the ability to become secreted from the cell (72). It has been shown that cholesterol binds to and dissociates from NPC1 and NPC2 at a faster rate when both proteins are present and functioning (49).

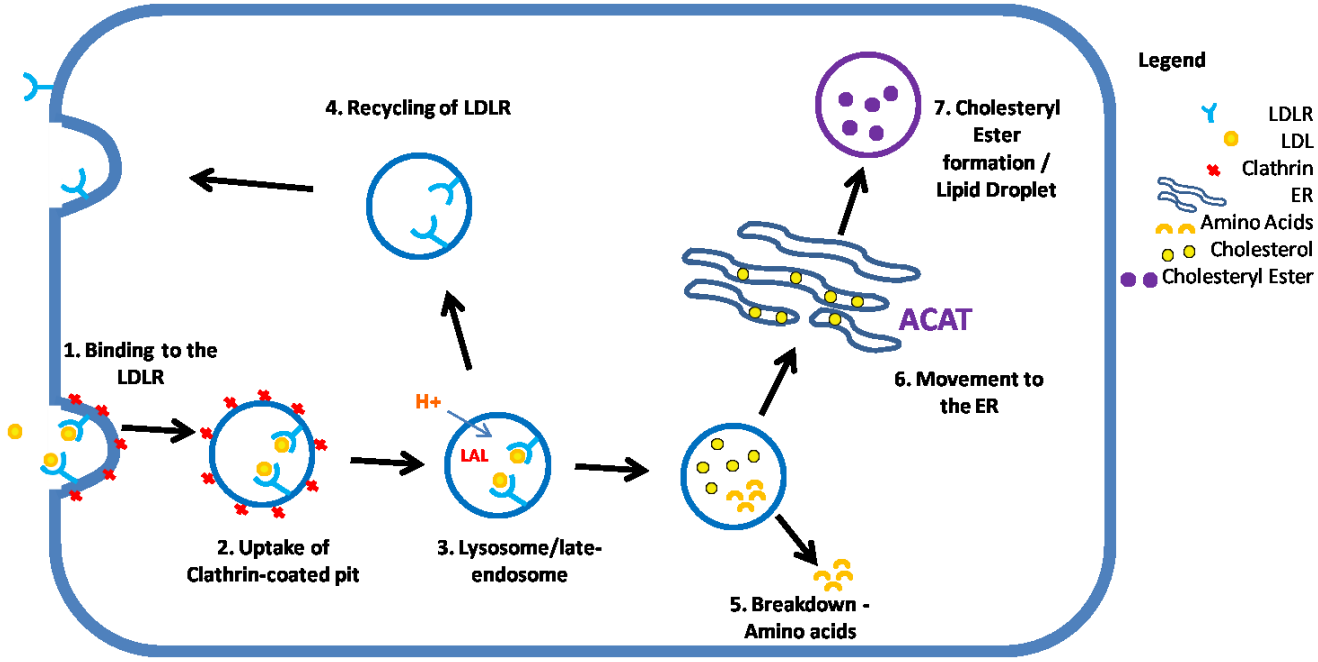

Figure 1.1. LDL Uptake Pathway. 1. LDLR is activated by SREBP and localized to the plasma membrane where it binds to LDL. 2. The LDL/LDLR complex is internalized in clathrin coated vesicles which fuse with early endosomes. 3. Within lysosomes/late endosomes, lysosomal acid lipase (LAL) breaks down the LDL into its basic components: cholesterol and amino acids. Endosomes mature to become lysosomes, with the pH becoming more acidic. 4. The LDLR is recycled back to the cell surface. 5. LDL is degraded in lysosomes, liberating free cholesterol, fatty acids, phospholipids and amino acids. 6. Cholesterol is transported to the ER via NPC1 and NPC2. 7. ACAT esterifies the hydroxyl group on cholesterol, creating cholesteryl ester, a storage form of cholesterol. In the ER, regulatory machinery causes the down regulation of LDLR and HMG-CoA Reductase genes and the increase of ACAT to accommodate the newly acquired cholesterol.

1.3.2 The NPC Hand-Off Model

Recent studies have used X-ray crystallography to generate structural models of cholesterol binding to these two proteins. Due to the hydrophobic properties of the cholesterol molecule, its mode of transport out of the lysosome was unknown. This new data has demonstrated that NPC1 and NPC2 work cooperatively in a 'hand-off' model (57). The model proposes that cholesterol binds to the NPC2 protein in an orientation that leaves the hydrophilic hydroxyl group free; it has been shown that NPC2 can bind both cholesteryl ester and free cholesterol in this manner. In addition, it has been shown that NPC2 is not sufficient to traffic cholesterol. This has been attributed to the orientation in which NPC2 holds the cholesterol molecule. This orientation has the hydrophobic region of cholesterol within the NPC2 protein and leaving the hydrophilic region free, which would make it unfavorable for movement through the hydrophobic lysosomal membrane. The cholesterol is transferred to the transmembrane NPC1 protein from NPC2, with the hydrophilic side chain buried within the NPC1 protein, allowing an easy passage through the membrane bilayer of the lysosome, with the hydrophobic region leading the way (57). This model is summarized in **Figure 1.2**, which is taken from the Goldstein and Brown group who led the way in this profound discovery. A stable structure of NPC1 and NPC2 during this 'hand-off' has yet to be observed, thus suggesting that the cholesterol transfer between the two proteins involves a short-lived interaction.

1.3.3 Cyclodextrin and NPC disease

Additional understanding of NPC disease comes from the recent usage of a compound that seems to overcome the phenotypic lysosomal blockage. 2-hydroxypropyl-β-

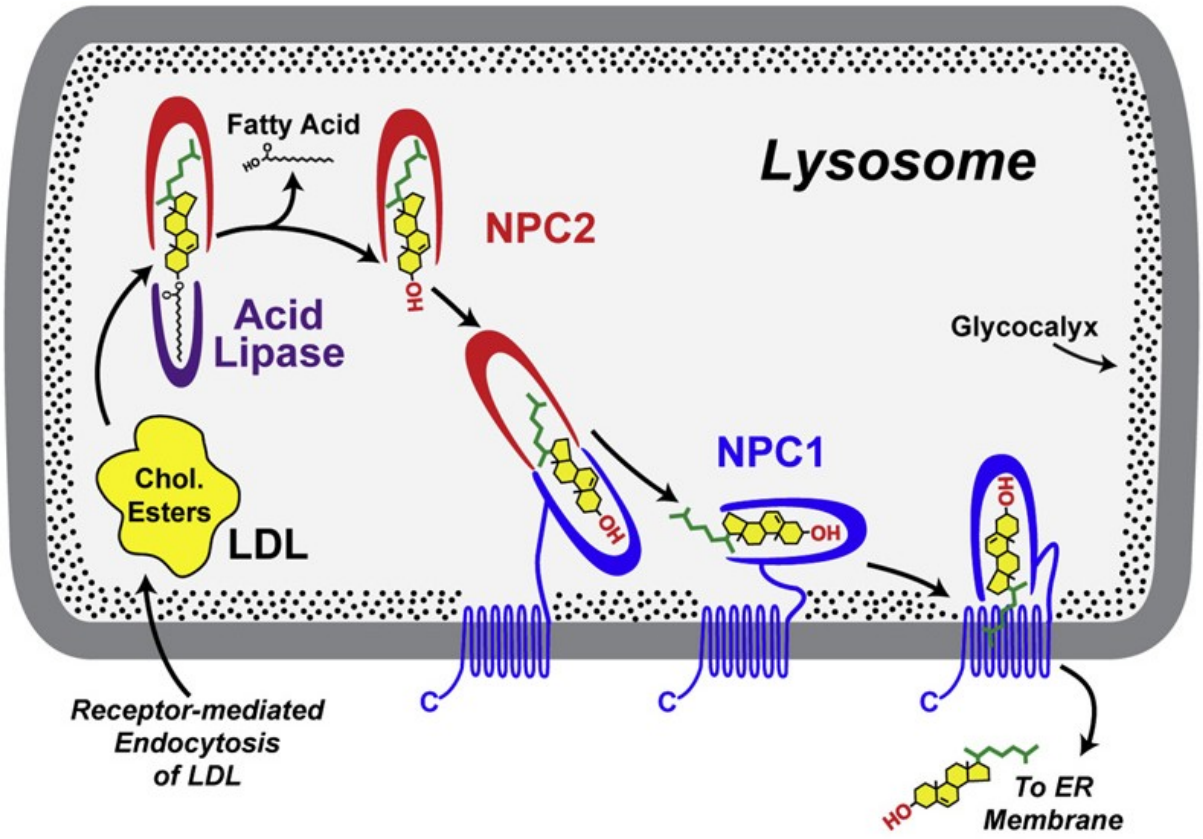

Figure 1.2. NPC1 and NPC2 'Hand-Off' Model. The proposed method of cholesterol transfer within the lysosomal compartment. NPC2 binds to the cholesterol or CE molecule in an orientation that leaves the hydroxyl group exposed. The cholesterol is then transferred to the transmembrane NPC1 protein in the opposite direction. This allows the hydrophobic edge of the cholesterol to lead the movement through the lysosomal lipid bilayer. The exact mechanism of movement through the lipid bilayer is still being examined. Image borrowed from Kwon., et al. (2009) (57).

cyclodextrin (cyclodextrin) is a large hydrophobic molecule that contains a lipophilic 'pocket' that has the ability to trap cholesterol (as well as other hydrophobic molecules) and extract it from either the lysosomes or plasma membranes, depending on the concentration used. When used in mouse studies in mice expressing *NPC1* mutations, this compound allows the egress of cholesterol from the lysosomal compartments, prolonging the life expectancy of the mice (66). The exact mechanism of how cyclodextrin bypasses the NPC1 and NPC2 proteins is yet to be determined. It is possible that the cyclodextrin enters the lysosomes through fluid-phase endocytosis and initiates cholesterol transfer from within the lysosomes (81). Alternatively, it is possible that cyclodextrin acts on the outside of the cell to remove plasma membrane cholesterol which, in turn, facilitates cholesterol movement from upstream membranes, including the lysosomes (75).

1.3.4 Alternate Models to overcome the effects of NPC Protein Impairment

While cyclodextrin remains the forerunner for potential use in medical therapies for reversing the adverse effects of NPC disease, several other lines of research have also shown promise. ATP-binding cassette transporter A1 (ABCA1) is a lipid transporter responsible for HDL particle formation and cholesterol efflux from the cell. Increase in this process is correlated with a decrease in the risk for cholesterol related diseases. It has previously been shown that cells harboring NPC mutations have decreased expression of the ABCA1 transporter (23). This was the first report of impaired transporter function that was not due to a mutation within the ABCA1 protein. This led to the hypothesis that restoring the cells with normal levels of this efflux machinery may be sufficient to reverse the lysosomal cholesterol accumulation seen in NPC cells. Treating NPC cells with a liver X receptor

(LXR) agonist, a positive regulator of ABCA1, restored activity of ABCA1 to near normal rates. This restoration was in turn able to reverse the lipid loading effects of NPC functional impairment (10). It was later shown that this efflux is dependent on the functionality of the NPC2 protein and not NPC1 expression (9).

In normal cells within the body, the cholesterol within lysosomes would be trafficked out of the cell with the help of several Rab GTPase proteins. Rabs are a family of GTPase enzymes that can bind to and hydrolyse guanosine triphosphate (GTP) and are involved in vesicle trafficking at various cellular sites, mainly within endosomes. It was shown that ubiquitously over expressing Rab 4, 7, 8 or 9 in mice can reduce the lipid accumulation seen in NPC mutant cells (24, 25, 65). This data prompted the generation of an *in vivo* model in which Rab 9 protein was over expressed in conjunction in NPC1 knockout mice. These mice had a longer life expectancy then their NPC1 knockout controls (54). These results, taken together with the success of the ABCA1 agonist study and with the studies proving the efficacy of cyclodextrin, provide solid evidence for attenuation of the defects in NPC via pathway regulation.

1.4 Cholesterol Regulation

1.4.1 Mechanisms of Cholesterol Regulation

Due to the importance of cholesterol, its regulatory machinery, including LDLR, is intricately balanced and well regulated. This regulation occurs by negative feedback regulation via the sterol regulatory element binding protein (SREBP) family and the resultant pathway for activation of these membrane-bound transcription factors (**Figure 1.3**) (14).

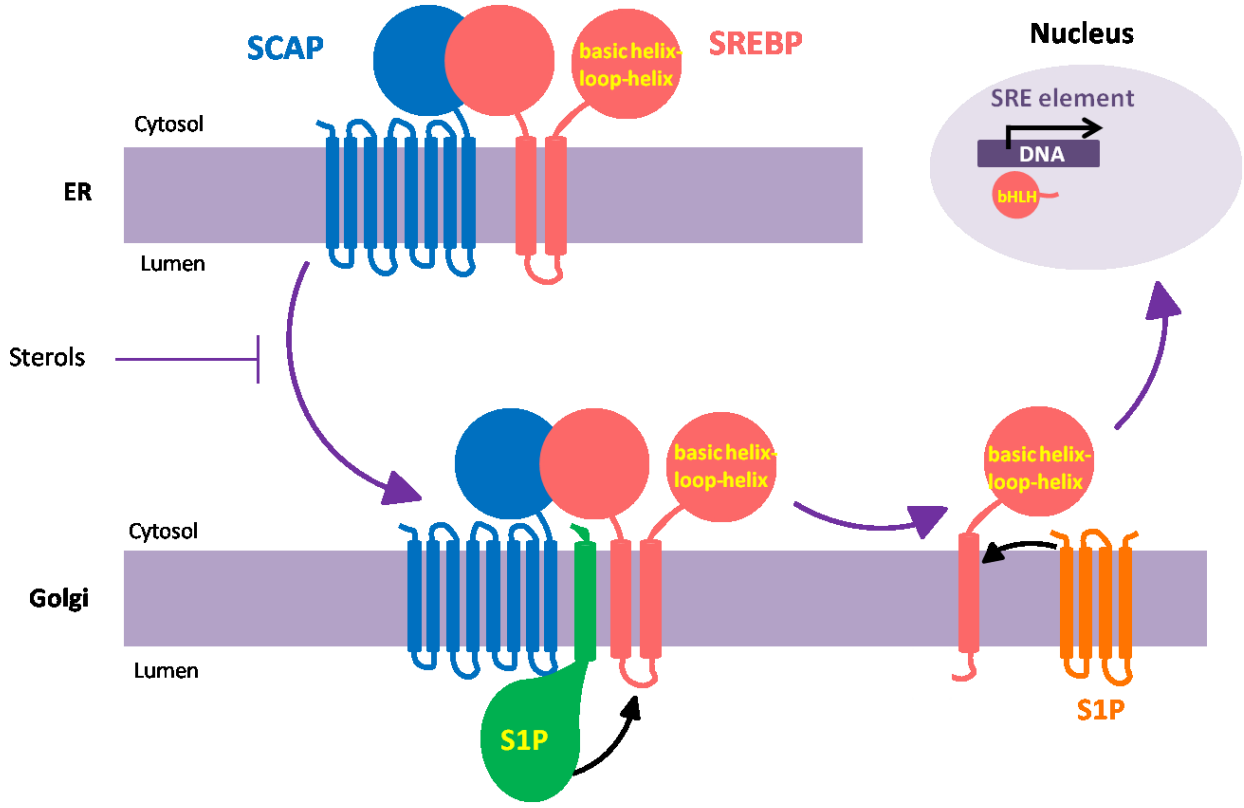

Figure 1.3. The SREBP Pathway. SREBP, the transmembrane transcriptional element, is located on the ER membrane with its N and C terminals pointing towards the cytoplasm of the cell. During sterol deplete conditions the SREBP chaperone protein SCAP is available to transport SREBP to the Golgi. Here, SREBP undergoes two proteosomal cleavages. The transcriptional element of SREBP, located in the bHLH domain, is then free to translocate to the nucleus where it binds to SRE elements in target genes and up-regulates the mRNA transciption of the cholesterol regulatory machinery, including LDLR, HMG-CoA reductase, and ACAT. Image modified from Brown and Goldstein (2009) (13).

1.4.2 SREBP Transcription Factors

The initial factor leading to the discovery of this regulatory pathway came when a sterol regulatory element (SRE) was discovered in the LDLR promoter sequence (87). It was later determined that there is a 10 base pair (bp) sequence to which the transcription factor SREBP can bind to as a dimer. This binding consequently promotes the transcription of LDLR when cells are sterol depleted and, therefore, require more cholesterol. This up-regulation of the LDLR will help the cell to take up the necessary cholesterol via LDL. This system is inactive when cells have sterols available, so as to avoid cholesterol toxicity. The SRE element was later shown to regulate multiple genes involved in cholesterol homeostasis. For example, the ER tethered enzyme 3-hydroxy-3-methylglutaryl-coenzyme A reductase (HMG-CoA reductase), the rate limiting enzyme in the endogenous production of cholesterol, also contains a SRE element within its promoter (16).

SREBP exists in two major forms, SREBP-1 and SREBP-2,(48) which are encoded by the genes *SREBF-1* and *SREBF-2*, respectively. SREBP-1 can be activated by two distinct promoters, which will produce either SREBP-1a or SREBP-1c via alternate splicing (85). These factors also play roles in the modulation of insulin regulation and TG synthesis (97). SREBP-1c is the predominant isoform in the liver, as well as adipose tissue. SREBP-2 is the main factor responsible for cholesterol homeostasis in the liver and is ubiquitously expressed. Ultimately, these transcription factors are enlisted to promote fatty acid synthesis in addition to their effects on cholesterol metabolism.

The process of SREBP regulation occurs during sterol rich conditions at which point the transcription factor is located in the nuclear and endoplasmic reticulum (ER) membranes. It is held here by its two membrane spanning helices. Due to its hairpin

formation, both the N and the C-terminals are located in the cytoplasm of the cell; the N terminal consists of a basic helix-loop-helix (bHLH)-Zip domain. SREBP cleavage-activating protein (SCAP), which is an eight membrane spanning transmembrane protein, plays a major role in trafficking of SREBP by acting as a chaperone protein (12). The C-terminus of the SCAP protein also projects into the cytoplasm and is able to mediate the protein-protein interaction between SREBP and itself, thereby maintaining the localization of SREBP in the ER during sterol rich conditions (**Figure 1.3**). SCAP will escort SREBP from the ER to the Golgi during sterol deplete conditions, through recruitment of the SCAP/SREBP complex into COPII mediated transport (89).

1.4.3 Insig-1 and the active SREBP Protein

SCAP on its own is not sufficient for the retention of SREBP within the ER; co-precipitation (Co-IP) studies with SCAP and SREBP identified that there was indeed another player involved (89, 90, 100). This element has been identified as Insig (insulin-induced gene)-1 and binds to the SCAP/SREBP complex to prevent its premature translocation to the Golgi. During cholesterol depletion, SCAP will undergo a conformational change, allowing its dissociation from Insig-1 and resulting in the proper translocation of SREBP to the Golgi.

Cholesterol and oxysterols have been shown to have separate physical effects on the SCAP protein. Cholesterol binds directly to SCAP, causing a conformation change that allows Insig-1 to bind to SCAP. In contrast, oxysterols are able to bind directly to Insig-1, causing a conformational change that allows it to bind to SCAP (**Figure 1.4**) (78).

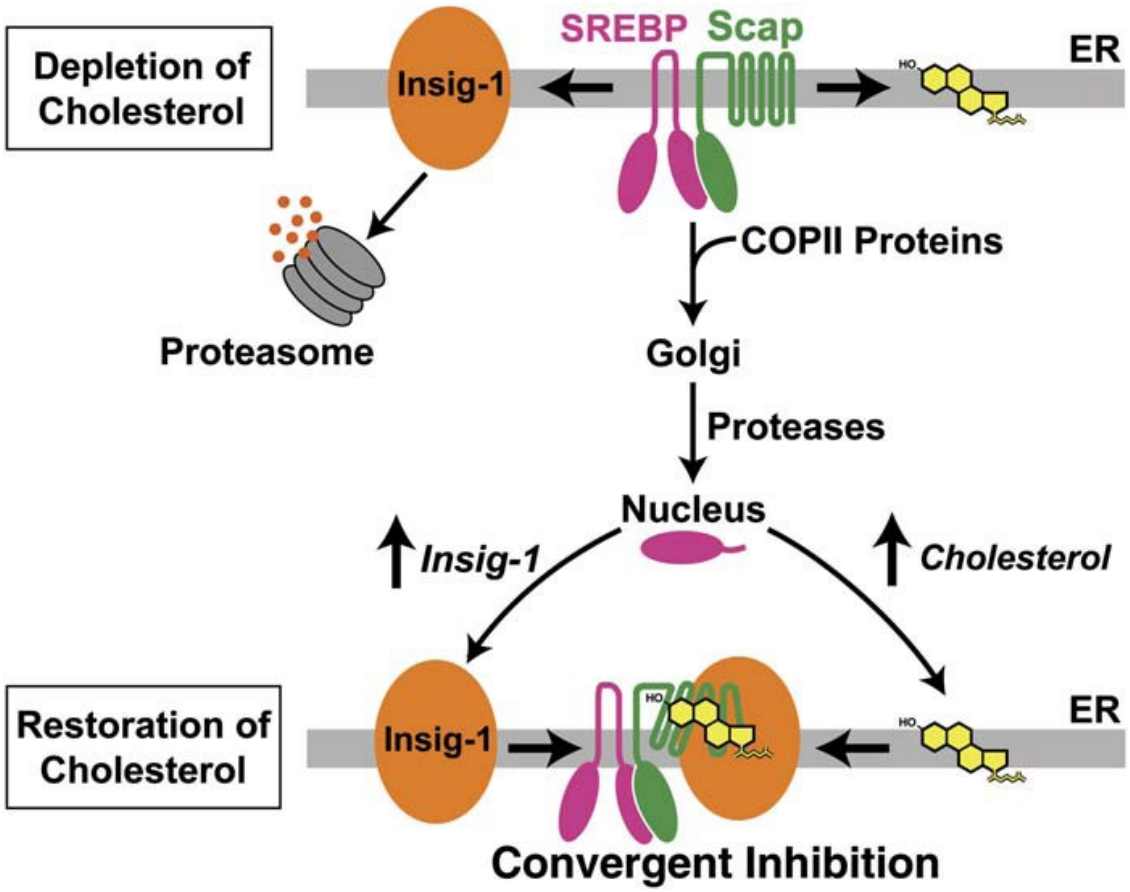

Figure 1.4. Cholesterol Regulation and Insig-1. SREBP, the transmembrane transcriptional element, is located on the ER membrane with its N and C terminals pointing towards the cytoplasm of the cell. The processing of SREBP as an active transcriptional element will only occur under cholesterol deplete conditions. When cholesterol is available to the cell, the Insig-1 protein will bind to SCAP due to a conformational change initialized by cholesterol. This will cease the necessary chaperone activity of SCAP, causing SREBP to remain bound to the ER. Image borrowed from Gong et al. (2006) (42).

The stoichiometric regulation offered by Insig-1 renders SCAP incapable of chaperoning SREBP from the ER to the Golgi during cholesterol rich conditions. When the Insig-1 protein is not bound to a SCAP/SREBP complex, it is rapidly ubiquitinated and degraded via the proteasome (42). When the SCAP/SREBP complex is able to translocate to the Golgi under sterol depleted conditions, Site-1 and Site-2 proteases (S1P and S2P, respectively) cleave the SREBP protein and release the active N-terminal complex; this complex is free to translocate to the nucleus to bind to the SRE elements (**Figure 1.3**). *INSIG-1* is also regulated by this pathway and is transcribed under sterol deplete conditions. Insig-1 is degraded until it binds to a SCAP/SREBP complex under cholesterol rich conditions, continuing the cycle. This method of regulation ensures that the cell will not unnecessarily terminate SREBP processing, as both Insig-1 and cholesterol are needed to maintain SREBP in its inactive state (42).

1.5 ACAT and the Lipid Droplet

Acyl-CoA:cholesterol acyl transferase (ACAT) is also regulated via the SREBP pathway and cholesterol homeostasis. ACAT is an enzyme located within the ER that is activated during times of excess cholesterol absorption; it functions in the conversion of cholesterol to its storable form: cholesteryl ester (60). From here, the cholesteryl ester will be stored within a lipid droplet. The lipid droplet is an organelle that consists of a hydrophobic TG and cholesteryl ester core surrounded by a phospholipid monolayer. It is thought that the lipid droplet originates from the ER. Several proteins are known to be associated with this dynamic organelle, including the family of PAT (perilipin, adipocyte differentiation-related protein (ADRP), and tail-interacting protein of 47 kDa (TIP47))

proteins (See Ref. 7 for a full review). These proteins are known to regulate the access of other proteins, such as lipases, to the materials within the lipid droplet core, as well as facilitating lipid droplet generation (7). Cholesterol in the lipid droplet can be incorporated into cellular membranes or undergo efflux from the cell via ATP-binding cassette transporters, such as ABCA1. Increased cholesterol efflux has been wildly associated with a decreased risk for cholesterol related diseases such as atherosclerosis (33, 38, 67).

1.6 Phosphatidylcholine

1.6.1 The CDP-Choline Pathway and Phosphatidylcholine

Phosphatidycholine (PC) consists of a glycerol backbone, polar choline head group and two fatty acid chains and is the most abundant phospholipid in eukaryotic cellular membranes (29). PC is used in hepatocytes for countless pathways, including the proper secretion of VLDL, as part of the layer encompassing lipid droplets, and as a major component in HDL, which acts to eliminate excess cholesterol from the cell (80). PC also plays major role in the structural integrity of the cell. Not surprisingly, a loss of PC is lethal to the cell (27, 32).

The production of PC is native to all nucleated cellular types. PC can be obtained from two pathways: through the cytidine diphosphate (CDP)-choline pathway (also known as the Kennedy Pathway), or through the methylation of phosphatidylethanolamine (PE) by phosphatidylethanolamine *N*-methyltransferase (PEMT). The former pathway accounts for approximately 70% of hepatic PC and uses choline as its initial substrate (29). It was recently shown that mice are able to synthesize choline *de novo* via PEMT (50). In all other cell types, the PC is obtained solely from the CDP-choline pathway. Choline is acted on by

three enzymes: choline kinase, CTP:phosphochilone cytidylyltransferase (CCT)α and cholinephophate transferase to generate PC (**Figure 1.5**). These enzymes use adenosine triphosphate (ATP), cytosine triphosphate (CTP), and diacylglycerol (DAG) as their consumption substrates, respectively. CCTα is the rate limiting step in this process, (55) with the degradation of PC chiefly mediated by calcium-independent phospholipase A2 ($iPLA_2$). This enzyme cleaves the PC molecule at the sn-2 position, creating a lysophosopholipid (lyso-PC) and a free fatty acid (2, 4). Lyso-PC can then be further degraded, generating glycerophosphorylcholine (GPC), which is largely excreted from cells. It is important to note that lyso-PC can be reacylated to become PC through the Lands pathway (76).

In addition to the role of PC as an essential structural component of cellular membranes, the breakdown of PC is important to the cell as it yields important molecules, such as arachidonic acid, phosphatic acid (PA), and DAG, that are involved in cell signaling events and are precursors for a variety of molecules. In addition to the breakdown achieved by $iPLA_2$, PC can also be hydrolyzed by either phospholipase C or phospholipase D, producing PA or DAG, respectively (46).

1.6.2 The Delicate Balance between Cholesterol and Phosphatidylcholine

Excess unesterified or free cholesterol can be toxic to the cell and can cause cell apoptosis, cell rigidity, ER stress, and cholesterol crystallization (86). The mechanisms that prevent this toxicity include cholesterol efflux as well as the many regulatory mechanisms highlighted in the above discussions. The orientation and makeup of the cellular membrane is essential to the maintained existence of a cell. PC molecules naturally adapt to a lipid

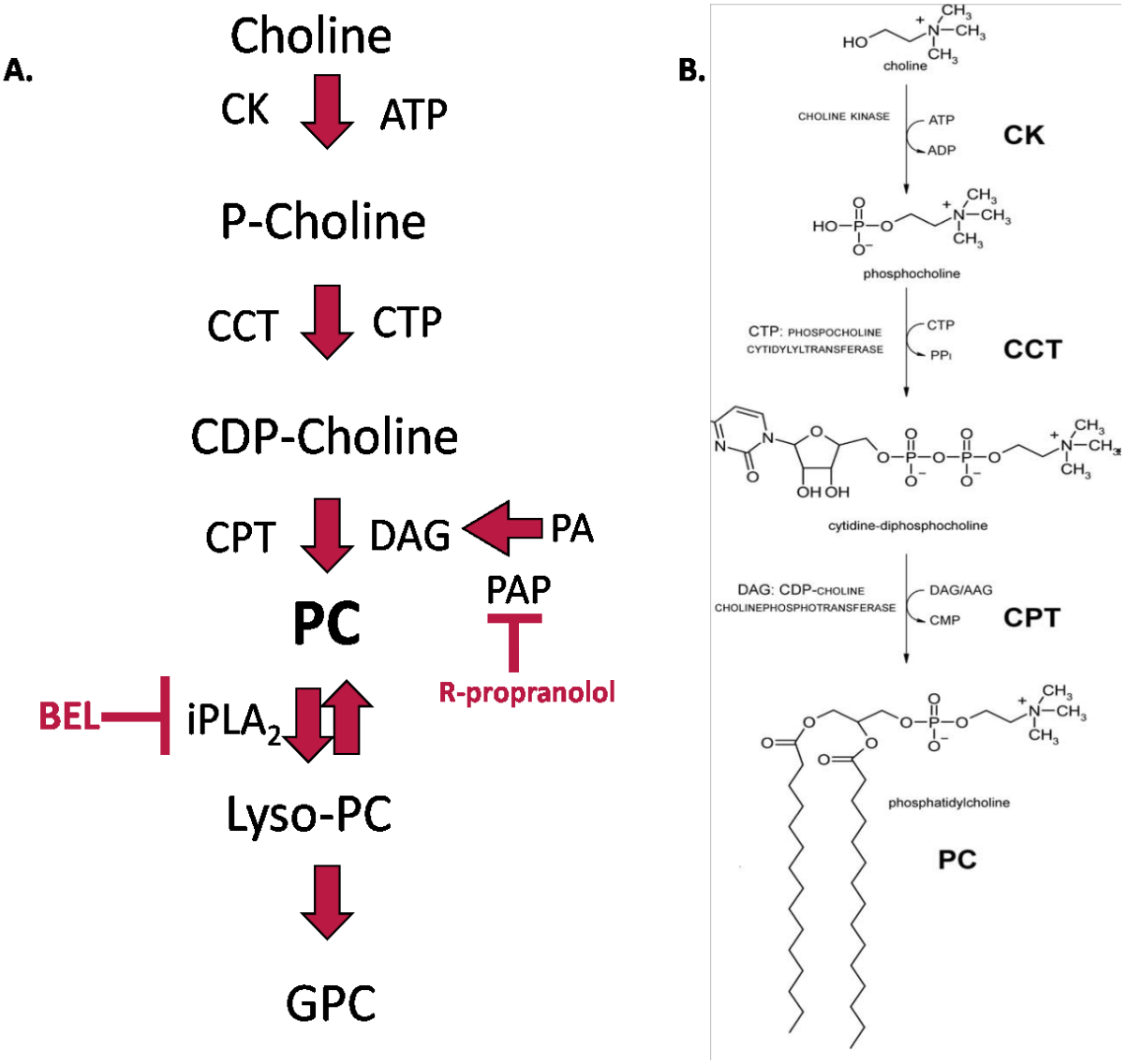

Figure 1.5. The CDP-Choline (Kennedy) Pathway. (A) The CDP-choline pathway is the primary source for the synthesis of PC in mammalian cells and tissues. The rate limiting step involves the conversion of P-choline to CDP-choline by the enzyme, choline-phoshate cytidylyltrasnferase (CCT)α. The enzyme choline phosphotransferase uses DAG as a substrate during the terminal step in PC synthesis. The breakdown of PC involves the cleavage of a fatty acid side chain to create lyso-PC, which is then degraded further. Several compounds that can be used to modify this pathway are shown, such as BEL and R-Propranolol. (B) The CDP-choline pathway in more detail. Image borrowed from Gibellini and Smith (2010) (37).

bilayer in solution, (43) with the non-polar tails pointed inwards and the polar heads towards the solvent (69). Cholesterol is able to fit within these PC molecules and affect membrane fluidity. Unsaturated PC alkyl chains tend to have a 'fluidizing' effect, opposite to the ordering or 'rigidifying' effect of cholesterol (88).

The molecular ratio of PC to cholesterol within the cell is of extreme importance and is therefore maintained within a narrow range (79, 92). A correlation between an increase in intracellular cholesterol and the rate of synthesis of PC has been reported numerous times (26, 58, 76). In particular, it has been shown that elevated cellular cholesterol levels cause an increase in the posttranscriptional activation of CCTα in cholesterol loaded macrophages (foam cells). It was also shown that this increase in CCTα correlates with the formation of membrane 'whorls'. These can be visualized by electron microscopy and are thought to act as a 'sink' to absorb the excess cholesterol within the cell. This overall effect would work to decrease the toxic effect of the cholesterol to the cell (86). It has alternatively been shown that cells lacking CCTα are more susceptible to cholesterol induced apoptosis then their wild type cell lines (102). This is due to ER-calcium depletion leading to ER stress and, ultimately, the expression of apoptotic pathways.

1.7 Sterol Regulatory Defective Cells

The studies presented use three distinct cell lines developed in the Goldstein and Brown laboratory, all derived from Chinese Hamster Ovary (CHO)-7 cells. Sterol regulatory defective (SRD) cells were created with the intention of studying cholesterol regulatory dysfunction and are summarized in **Figure 1.6**. Several SRD cell lines were created; the two employed for this work are SRD-2 and SRD-4 cells. The SRD-2 cell line was generated

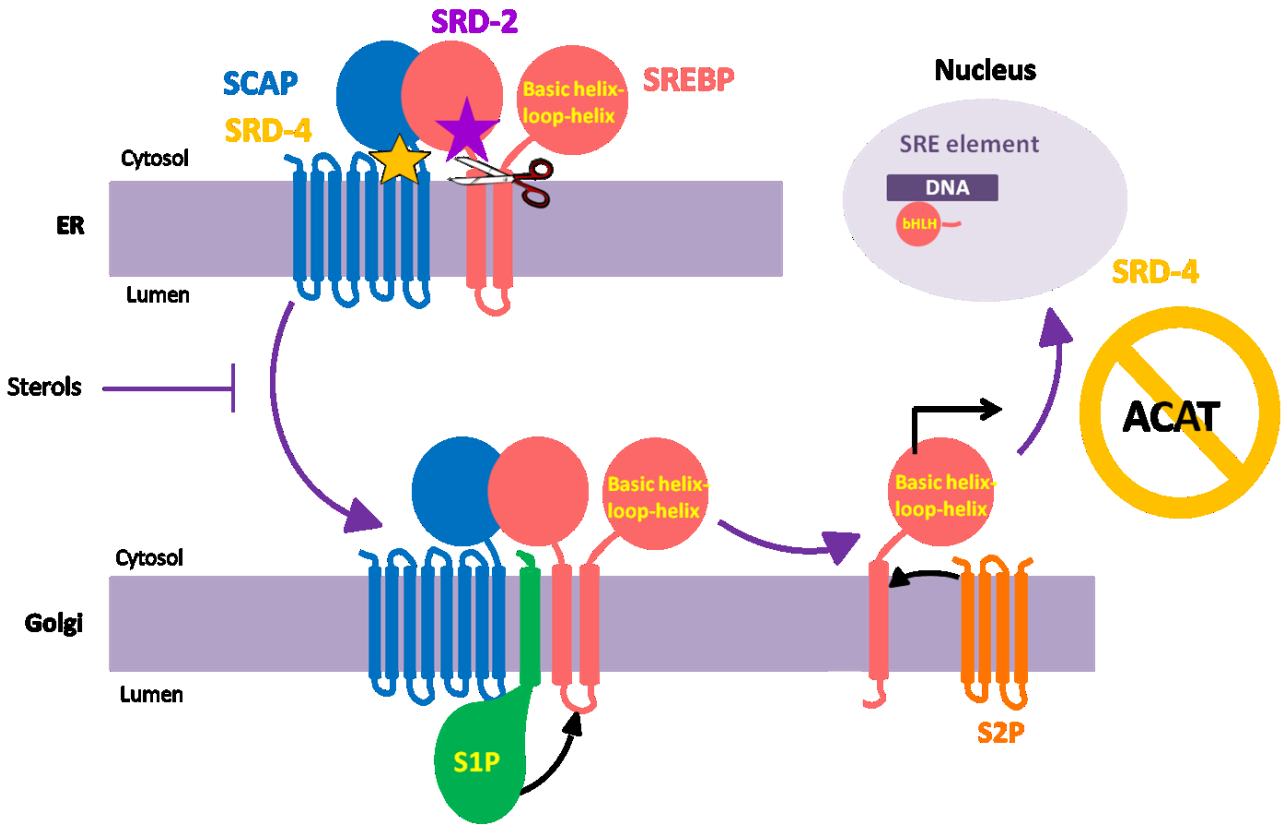

Figure 1.6. Sterol Regulatory Defective (SRD) Cell Line Mutations. Three distinct cell lines were employed in this thesis. The parental cell line used was of Chinese hamster Ovary (CHO) origin, specifically, CHO-7 cells adapted for long-term growth in medium containing lipoprotein-deficient serum. Two sterol regulatory defective (SRD) cell lines were mutated from this parental line and selected for defective cholesterol metabolism by selection for resistance to 25-HC. SRD-2 cells carry a truncated version of the SREBP-2 protein, while SRD-4 cells have a point mutation (D443N) in the sterol sensing domain of the SCAP protein, as well as non-functional ACAT activity. Both of these cell lines constitutively upregulate SREBP target genes, regardless of sterol concentrations.

via γ-irradiation (99). They were subsequently selected for and maintained in 25-hydroxycholesterol (25-HC). 25-HC cannot be used as a substitute for cholesterol within the cell membrane; however, the cell senses the presence of this sterol as cholesterol and suppresses SREBP processing. As a result, wild type cells die due to insufficient cholesterol. It is the improper cholesterol regulation of the SRD-2 cell line that allows them to flourish despite the presence of 25-HC. It was determined that the defective cholesterol regulation in SRD-2 cells was due to a truncation at amino acid 460 of the SREBP-2 protein resulting in expression of the soluble transcription factor domain that is constitutively active (98). The SREBP-2 protein in the CHO-7 cells have a 93% identical sequence when compared to the human sequence (99). This similarity includes the vastly important sequence required for transcriptional activation.

The SRD-4 cell line was created from CHO-7 cells via mutagenesis with nitrosoethylurea and were selected for using 25-HC, in the same manner as selection for the SRD-2 cell line. It was determined that SRD-4 cells lack functioning ACAT activity (70). This was later shown to be due to a point mutation within one allele of ACAT that renders the enzyme inactive (20). Despite this mutation, the cells are able to maintain a normal rate of TG synthesis. Due to the lack of functional ACAT, these cells are not able to create cholesteryl esters in the presence or absence of cholesterol derived from LDL. The lack of ACAT enzyme activity is not the sole reason SRD-4 cells are able to thrive in 25-HC conditions. In addition, these cells have a dysregulation of the cholesterol sensing pathways due to a point mutation in SCAP (D443N) which renders it partially insensitive to cholesterol. Thus in SRD-4 cells there is increased and sterol-insensitive processing of both SREBP-1a and SREBP-2 (73, 47). Both SRD-2 and SRD-4 cell lines are unable to properly

modulate cholesterol intake and, as a result, continually take up cholesterol, regardless of the concentration of cholesterol within the cell.

A final note regarding the SRD-4 cell line highlights the co-regulation of cholesterol and PC metabolism. The rate of PC synthesis in the SRD-4 cells is greatly increased when compared to the parent CHO-7 cell line, due to increased synthesis of fatty acids mediated by chronic SREBP activity. This, in turn, positively regulates CCTα, the rate-limiting enzyme in the CDP-choline pathway. Despite this increased rate of synthesis, the overall PC mass of the cells is not greater than that of the CHO-7 cell line, as a result of increased catabolism of the PC molecules (58). Overall, these cells provide an interesting platform for cholesterol metabolism studies.

1.8 Research Objectives

Understanding the cholesterol pathway in its entirety is a daunting task that has captivated researchers for years. The primary goal of the presented research is to determine the influence of an altered PC to cholesterol ratio on the egress of LDL-derived cholesterol from the lysosomal compartments. More specifically, this work looks at whether PC can enable the egress of cholesterol out of the lysosomes during cholesterol over-loading. The ratio of PC to cholesterol is vastly important, and we hypothesize that when this ratio is thrown off due to cholesterol over-loading, free cholesterol will be sequestered within lysosomal compartments in order to prevent cholesterol toxicity to the cell. By manipulating the CDP-choline pathway we have observed that increasing the available cellular PC can indeed positively influence the movement of cholesterol out of the lysosomal compartments. In the same manner, we have observed that decreasing the cells

ability to make PC, via inhibition of the synthesis of a needed substrate, can also create a lysosomal blockage. This inhibition of cholesterol movement can be alleviated by providing the cell with exogenous means to increase cellular PC. In addition, we have examined the possibility that normalizing the PC to cholesterol ratio specifically in the ER through regulation of ACAT activity can influence the cholesterol movement out of the lysosomes. Understanding what triggers the movement of cholesterol from the lysosomes can lead to a greater understanding of cholesterol metabolism as a whole.

2 Material and Methods

2.1 Preparation of Lipids and Serum

2.1.1 Preparation of Lipoprotein Deficient Serum

Lipoprotein-deficient serum (LPDS) was prepared from fetal bovine serum (FBS). 28 mL of FBS, with the density adjusted to 1.21 g/mL with dried potassium bromide (KBr), was added to 40 mL centrifuge tubes (Beckman). An overlay of 1.21 g/mL of KBr density solution, made in ddH_20, was used to fill the remaining volume. Tubes were then subject to centrifugation in a 55.2 Ti rotor (Beckman) at 44,000 rpm for 39 hours using a Beckman L8-70M Ultracentrifuge. The upper lipoprotein fraction was partitioned by tube slicing and the lower LPDS fraction (d > 1.21 g/ml) was dialyzed extensively against PBS (pH 7.4, 137 mM NaCl, 2.7 mM KCl, 2.0 mM KH_2PO_4, 14.4 mM Na_2HPO_4, pH 7.4) for six washes over three days. LPDS was then filtered-sterilized and stored in aliquots at -20^{o}C.

2.1.2 Preparation of Low-Density Lipoproteins

Low-density lipoprotein (LDL) was prepared from fresh blood collected from healthy donors into EDTA tubes, followed by low-speed centrifugation at 3,500 rpm for 20 minutes at 4^{o}C. Cleared plasma was removed to a fresh tube, and the density was adjusted to 1.019 g/ml using KBr. The samples were centrifuged for 18 hours at 55,000 rpm in a 70 Ti rotor (Beckman). The upper portion of the tube containing VLDL and IDL was partitioned by tube slicing and the lower fraction collected for further processing. The lower portion was then readjusted to a density of 1.063 g/ml with KBr and centrifuged for 18 hours at 58,000 rpm in a 55.2 Ti rotor. LDL was collected and dialyzed against PBS-EDTA (PBS pH 7.4, 125 μM EDTA) for six washes. Protein concentration was determined with a modified Lowry protein assay (77).

2.2 Modified Lowry Protein Assay

Solution A consisted of equal parts copper-tartrate-carbonate (CTC), 10% SDS and 0.8 N Sodium Hydroxide. CTC is made up of 20% sodium carbonate added to an equal volume containing 0.2% copper sulfate (petahydrate) and 0.4% potassium tartrate. Solution B consisted of Folin-Ciocalteu phenol reagent diluted 1:5 in ddH_20. The sample was mixed with ddH_20 to a final volume of to 400 µL (typically 5-25 µL of sample, depending on concentration). Standard curves were prepared using a BSA reagent with concentrations ranging from 2-20 µg/mL. 400 µL solution A was added to all samples, and allowed to sit for 10 minutes at room temperature. 200 µL of solution B was added and allowed to sit for 30 minutes. Absorbance was read at 660 nm on a BIOWAVE II spectrometer (Biochrom Ltd.,) and plotted against the determined standard curve.

2.3 Cell Culture

SRD-2 and SRD-4 cells were maintained in Dulbecco's high glucose modified Eagle's medium (DMEM) with 5% LPDS, 100 U/ml penicillin and 100 µg/ml streptomycin, 33 µg/ml proline, 3.0 µg/ml 25-hydroxycholesterol (25-HC), and 0.2% FBS (medium A). CHO-7 cells were cultured in DMEM containing 5% LPDS, 100 U/ml penicillin and 100 µg/ml streptomycin, 33 µg/ml proline and 0.5 % FBS (medium B). For experiments, all three cell lines were subcultured in medium B in the absence of FBS. Cells were maintained in an environment of 5% CO_2 at 37 ^oC.

2.4 Cell Treatments

Cells were cultured to ~70% confluency prior to the start of treatments with the various compounds. In all cases, optimal doses were determined in preliminary experiments (data not shown). Bromo-enol Lactone (BEL; Cedarlane) was dissolved in dimethyl sulfoxide (DMSO) and used at a concentration of 25 μM. Cells were treated with a 1 hour pretreatment prior to the longer 20 hour treatments, in the absence or presence of LDL. R-Propranolol (Prop; Sigma) was dissolved in DMSO and used at a concentration of 60 μM for 20 hour treatments. L-a-lysophosphatidylcholine (lyso-PC; Avanti Polar Lipids) purified from an egg source was purchased in chloroform, dried with a stream of nitrogen, dissolved in PBS and sonicated under 10% output conditions for 15 second pulses six times, with 5 second breaks. The test tube was kept in water during sonication to avoid overheating. Lyso-PC was used at a concentration of 50 μM for 20 hour treatments. ACAT inhibitor (ACATi; Sandoz) product 58-035 was used at a concentration of 2.5 μg/mL. Cells were either treated for 20 hours and stained with filipin, or treated for 20 hours plus a washout time and then stained with filipin. During the washout (4-8 hours), cells were incubated with the standard experimental medium. Methyl β-cyclodextrin (CD; Sigma) was dissolved in ddH_20 and used at a concentration of 1.5 mM during a 4 hour treatment before filipin staining. The compound U18666A (BIOMOL) was used in 20 hour incubations at a concentration of 1 μg/mL.

2.5 Microscopy

2.5.1 Filipin Staining and Quantification

Cells were plated on cover slips at 80,000 cells/well in a 12-well plate, on day one. On day two cells were treated, as described in *2.4 Cell Treatments*. On day three, cells were washed twice with PBS and then incubated with 4% paraformaldehyde (PFA) (0.8g PFA, 0.25 μM NaOH, PBS, pH 7.5) for 30 minutes at room temperature. After removal of PFA cells were washed for 10 minutes with 1.5 mg/mL glycine in PBS. Filipin complex (Sigma) was diluted in DMSO and incubated with the cells at a concentration of 25 μg/mL for 30 minutes. Filipin stain is specific to unesterified cholesterol, such as that contained within the lysosomal compartments. Cells were washed in PBS three times for 5 minutes each. For quantification purposes, cells were stained with the cell-permeable DNA stain DRAQ5 (5 μM; BioStat) for 15 minutes. Cover slips were washed in PBS one final time. Cover slips were mounted on glass slides using Fluorescent Mounting Media (Dako) and left to dry at 4^{o}C overnight before viewing. Images were taken using the confocal microscope Fluoview FV1000 Version 2.1 (Olympus) and analyzed using FV10-ASW software. Filipin was visualized using a 405 nm laser, and a 633 nm laser was used for DRAQ5. Manual identification of a field was determined in the images and analyzed for intensity with Fluoview program software. The number of cells per field was counted and average intensity per cell was determined for each condition. A minimum of 5 fields per condition were analyzed.

2.5.2 Imunofluorescence microscopy

Cells were plated on coverslips at 80,000 cells/well in a 12-well plate, on day one. On day two cells were treated, as described in *2.4 Cell Treatments*. On day three, cells were washed twice with PBS and fixed in 3% formaldehyde-PBS immunofluorescence buffer (PBS-IF; 2 mM $MgCl_2$, 225 mM NaCl, 10 mM Na_2HPO_4, pH 7.4) for 15 minutes. Cells were then washed twice in PBS-IF containing freshly-prepared 5 mM ammonium chloride (NH_4Cl) before permeabilization with 0.05% (w/v) Triton X-100 for 10 minutes at -20 ^oC. Coverslips were allowed to air dry for 1 minute before being washed three times with PBS-IF. The cells were blocked in a solution of 1% BSA in PBS-IF for 30 minutes. Primary antibody incubations were performed in 1% BSA PBS-IF solution for 1 hour at 25 ^oC. The NPC1 primary antibody was used at a dilution of 1:250 (Novus Biologicals). Following primary antibody incubations, coverslips were washed three times for 15 minutes each in 1% BSA PBS-IF. Secondary antibody incubations were also performed in 1% BSA PBS-IF, using cross-absorbed 488 nm Alexafluor-conjugated secondary donkey anti-rabbit antibodies (Molecular Probes), at a concentration of 1:500. Coverslips were subjected to three 15 minute washes in 1% BSA PBS-IF. The final wash contained 2 µg/mL Hoechst 33342 (Life Technologies, Invitrogen). Coverslips were rinsed briefly in ddH_20 before being mounted with Fluorescent Mounting Media (Dako) and left to dry at 4^oC overnight before viewing with the confocal microscope. Hoechst was visualized using a 405 nm laser and Alexafluor was visualized using a 488 nm laser.

2.5.3 Nile Red Staining

Cells were plated on cover slips at 80,000 cells/well in a 12-well plate, on day one. On day two cells, were treated, as described in *2.4 Cell Treatments*. On day three, cells were washed once with PBS and incubated with 4% PFA for 10 minutes at room temperature. After removal of the PFA, cells were washed twice with PBS. Cells were stained for 30 minutes in the dark with Nile Red (Invitrogen) at a concentration of 1.0 μg/mL in PBS, made from a stock solution of 0.2 mg/mL in acetone. Nile red has been shown to be specific to highly hydrophobic lipids, such as those contained within the core of lipid droplets. Using this compound we are able to visualize these dynamic organelles. Cells were washed twice with PBS cells and stained with the cell-permeable DNA stain DRAQ5 (5 μM; BioStat) for 15 minutes. Cover slips were mounted on glass slides using Fluorescent Mounting Media (Dako) and left to dry at 4^{o}C overnight before viewing. Images were taken using the confocal microscope Fluoview FV1000 from Olympus using the 488 nm laser for nile red, and the 633 nm laser for DRAQ5.

2.5.5 Colocalization Studies

Cells were plated on cover slips at 80,000 cells/mL in a 12-well plate, on day one. On day two, cells were treated, as described in *2.4 Cell Treatments*. Cells were co-incubated with 1 mg/mL of Texas Red conjugated Dextran complex, 10,000 MW (Invitrogen). On day three, cells were washed and stained with filipin as described in *2.5.1 Filipin Staining and Quantification*. Images were taken using a wide-field fluorescence microscope (Delta Vision CORE; Applied Precision). Images were acquired using a 405 nm laser for filipin and a 594 nm laser for the Dextran complex. Co-localization was determined when areas of interest

showed significant staining of both the filipin and Dextran complexes. This was determined with merge images.

2.6 Western Blotting

2.6.1 Primary Antibodies

Rabbit polyclonal LDL-receptor (LDLR) antiserum 4548, raised against full-length bovine LDLR, was the kind gift of Dr. Joachim Herz (University of Texas Southwestern Medical Center, Dallas, TX). In addition, mouse monoclonal anti-actin AC-40 (Sigma) and polyclonal NPC1 antibody (Novus Biologicals) were used. All primary antibodies were used at a 1:1000 dilution in antibody dilution buffer (PBS - Tween (PBS, 0.1 % Tween 20), 5% BSA, and 0.02% NaN_3).

2.6.2 Western Blotting

Cells were plated at 900,000 cells/dish in a 60 mm plate, on day one. On day three, cells were treated with the appropriate treatments, as described in *2.4 Cell Treatments*. On day four, cell medium was aspirated and cells were washed twice with PBS at 4^{o}C. Cells were collected in 1.5 mL PBS and spun at 2,000 rpm for 5 minutes at 4^{o}C in a Legend Micro 17R Centrifuge (Sorvall). The supernatant was aspirated and cells were washed in 0.5 mL PBS and re-spun under the same conditions. Samples were resuspended in the appropriate volume of Lysis Buffer (50 uM Tris-Cl, pH 7.4, 150 mM NaCl, 1% TX-100, 0.5% sodium deoxycholate, 5 mM EDTA, 5mM EGTA) on ice, in the presence of 1 X Protease Inhibitors (Roche Diagnostics), for approximately 30 minutes. Samples were spun down for 15 minutes at 13,000 rpm at 4^{o}C to remove cell debris. Final samples were subject to a µLowry

protein assay and samples made up in 4X SDS-PAGE sample buffer (0.2 M Tris (pH 6.8), 4% SDS, 20% glycerol, 0.04 M EDTA (pH 8.0) 0.016 % Bromophenol blue). 0.28 M β-mercaptoethanol (BME) was added to each sample immediately prior to heating at 96 ^{o}C for 5 minutes. In all cases, 30 μg samples were run on a 30% acrylamide gel for approximately 1.5 hours at 120 V. Samples being probed with the NPC1 primary antibody were not heated prior to loading on the gel. The gel was transferred to a nitrocellulose membrane for 1 hour at 120 V. Following the transfer, the membrane was blocked in Blotto buffer (5% Newborn calf serum, 5% skim milk in PBS) and incubated with primary antibody, diluted 1:1000 in antibody dilution buffer, with shaking for 1 hour at room temperature or overnight at 4^{o}C. Secondary antibodies, either IRDye 800CW goat anti-rabbit IgG or IRDye 800CW goat anti-mouse IgG (LI-COR Biosciences), were diluted 1:4000 in Blotto buffer and left for 45 minutes at room temperature. Following primary and secondary antibody incubations, membranes were washed three times for 10 minutes each in PBS-Tween. Blots were scanned and visualized on a LI-COR Odyssey Infrared Imager, and the intensity of bands corresponding to proteins of interest was quantified using Odyssey 2.0 software. Samples were normalized to the actin protein concentration per lane.

2.7 Mass Cholesterol Assay –

Cells were plated at 90,000 cells/well in a 12-well plate, on day one. On day two, cells were treated with the appropriate conditions, as described in *2.4 Cell Treatments*. On day three, medium was aspirated and cells were washed twice with PBS. The cells were incubated with 250 μL of 0.05% trypsin at 37 ^{o}C for 10 minutes. Cells were collected, with an additional 0.25 mL of PBS to collect excess cells. Samples were spun at 2,000 rpm for 5

minutes at 4°C. The supernatant was aspirated, and the cells were resuspended in 60 µL of PBS. A total of 10 µL of each sample was used to determine a cell count, using the TC10 Automated Cell Counter (Bio-Rad). The remaining 50 µL sample was transferred to a test tube and spun at 3,000 rpm for 10 minutes at 4°C in a Sorvall Legend XTR Centrifuge. The supernatant was removed and samples were resuspended in 200 µL isopropanol and 1% Triton X-100 solution for 30 minutes at room temperature. Samples were spun for 15 minutes at 4,000 rpm at 4°C, and supernatants were collected. Samples were allowed to air dry for 2 days or for 15 minutes using a nitrogen stream. Samples were processed using the Cholesterol/Cholesteryl Ester Quantification Kit (BioVision). Briefly, samples were resuspended in 200 µL of cholesterol assay buffer. 50 µL and 20 µL of samples were added to a black 96-well plate (Costar Assay Plate, Fisher). Samples were incubated for 1 hour at 37 °C before being read on a Polar Star plate reader with an excitation of 535 nm and emission of 590 nm. Samples were standardized against a fluorescent cholesterol probe.

2.8 Flow Cytometry

Cells were plated at 300,000 cells/well in a 24-well plate, on day one. On day two, cells were treated with the appropriate conditions, as described in *2.4 Cell Treatments*, in the presence of 1.5 µg/mL of Dil-LDL (Invitrogen) or 300 µg/mL of non-labeled LDL for 3 hours. Cells were washed twice with PBS and left to incubate for 15 minutes at 37 °C in 0.5 mL lifting buffer (equal amounts of RPMI media (10% FBS) and 10 µM EDTA, pH 7.4). Cells were collected and filtered through a 70 µM sterile cell strainer (BD Biosciences). An additional 0.5 mL of PBS was used to collect excess cells from the wells. Samples were spun in 1.5 mL tubes at 2,000 rpm for 5 minutes at 4°C. Supernatant was aspirated and

samples were resuspended in 0.5 mL wash buffer (0.11% w/v EDTA, 0.1% FBS in PBS) and re-spun using the same conditions. The supernatant was aspirated, and samples were resuspended to a final volume of 0.25 mL of sterile PBS. Samples were processed using the BD FACSAria flow cytometer and cell sorter (BD Biosicences). Briefly, single cells are passed through a laser beam; those that have taken up the Dil-LDL will emit a fluorescence signal that will be detected by the flow cytometer at a wavelength of 571 nm. The overall population of cells that emit the signal will be counted and compared to the population of single cells that do not emit a signal.

2.9 Collection and Analysis of [^{3}H] choline-labeled metabolites –

Cells were plated at 900,000 cells/dish in 60mm dishes, on day one. On day two, cells were incubated with the appropriate conditions, as described in *2.4 Cell Treatments*. On day three, cells were incubated with 6μCi of ^{3}H labeled choline (PerkinElmer) in 2mL of complete media. After one hour of incubation, the cells were placed on ice and media removed. The cells were washed twice with cold PBS. A total of 1mL of MeOH:H_2O (5:4) was added to each dish and the cells collected. This was repeated with an additional 1 mL of the same solvent and the cells pooled. Finally, 1mL of the solvent was added to each test tube after collection. Samples were sonicated for approximately 10 seconds under 10% output with a needle-tip sonicator to break up cells. At this point, aliquots were removed to be used for a μLowry protein assay. To each tube, 4 mL of $CHCl_3$ was added. The samples were vigorously shaken for 10 seconds by hand or vortexed for 30 seconds. Samples were spun at 2,000 rpm for 5 minutes at 4 ^oC. A 1.5 mL aliquot of the upper phase was collected and used for future analysis (see continuation of protocol below). The protein layer and

remaining upper phase portion were removed and discarded. A total of 2 mL of Ideal Upper Phase (IUP) (45:47:3 MeOH:0.58% NaCl:$CHCl_3$) was added to the lower, organic phase. The sample was vortexed and centrifuged at 2,000 rpm for 5 minutes at 4 ^oC. The upper phase was aspirated and this step repeated a second time. The lower phase was kept and samples dried under a stream of nitrogen. These organic samples were resuspended in 1 mL $CHCl_3$ and vortexed. 50 µL aliquots of these samples were removed to scintillation vials and allowed to dry overnight in the fume hood. Samples had 3 mL scintillation cocktail (EcoLite (+), MP Biomedicals, LLC.,) added to each vial before being vortexed and read in a scintillation counter (Liquid Scintillation Analyzer – Tri-Carb 2100 TR, Perkin Elmer). Results normalized to protein levels. The organic phase contains more than 98% of PC counts following a 1 hour pulse-labeling with ^3H-choline (96).

The collected upper phase samples had 40 µl of 'upper phase mix' (2.5 mg/mL unlabelled choline, phosphocholine, CDP and GPC in MeOH:ddH_20 (1:1)) added to each sample before they were dried under a stream of nitrogen on a heating block of 37 ^oC. The samples were then resuspended in 100 µl of MeOH:H_2O (1:1) and vortexed. A total of 40 µl of each sample was spotted on a silica gel GHL plate (Analtech) and separated by Thin Layer Chromatography (TLC). This was done in a solution of Ethanol:H_20:ammonia (48:95:6) for approximately 2 hours or until the plate was 1 inch from the top. A total of 50 µg of each lipid to be analyzed was also run in a standard lane for comparison. The plate was dried overnight and stained with 1% stannous chloride in 3N HCl, followed by 1% phosphomolybdic acid in $CHCl_3$: EtOH (1:1). Visualized samples were marked and scraped into scintillation vials. To each vial, 250 µl of H_2O was added, and samples were vortexed

before the addition of 3 mL of scintillation cocktail, before an additional vortex of each sample and followed by counting. Samples were normalized to protein levels.

2.10 Statistical Analysis –

Statistical analysis was performed using SigmaStat 3.5 (SigmaStat, Systat Software Int., San Jose, CA). All analysis was performed using a One Way ANOVA.. Values are shown as mean ± standard deviation for at least 3 independent experiments. A $p < 0.05$ was considered significant.

3 Results

3.1 Cholesterol Accumulation and Alleviation with BEL

3.1.1 Cholesterol Accumulation in Sterol Regulatory Defective (SRD) Cell lines

Three cell lines were used in this study. The CHO-7 cell line is a Chinese hamster ovary cell line derived from CHO-K1 and adapted to long-term growth in lipoprotein-deficient serum. Two distinct Sterol Regulatory Defective (SRD) cell lines, SRD-2 and SRD-4 were derived from CHO-7 cells through chemical mutagenesis followed by selection for resistance to 25-hydroxycholesterol mediated cell-death (70, 99). As detailed in the Introduction, both SRD cell lines harbor mutations that render then incapable of regulating negative feedback control of cholesterol synthesis and LDL uptake. Both SRD cell lines were seen to accumulate unesterified cholesterol within lysosomal compartments when incubated with 50 μg/mL LDL for 20 hours (Figure 3.1, panels G and L). The fluorescent dye filipin, which binds unesterified cholesterol, was used to examine sites of accumulation of free cholesterol in cells, revealing accumulation in punctate cytoplasmic structures, consistent with lysosomes/late endosomes. Morphologically, this effect was greatest in the SRD-4 cells that lack functional ACAT activity. The CHO-7 cell line did not show this effect under the same conditions. These vesicular punctate structures were confirmed to be lysosomal via co-localization experiments using fluorescently-labeled dextran (MW 10,000 kDa) (Figure 3.2), a compound which is taken up via bulk phase endocytosis and sequestered in the lysosomes (39). This shows that both the SRD-2 and SRD-4 cells regulate their cholesterol regulatory pathway in an impaired fashion, and as a result of excess LDL uptake free cholesterol accumulates in the lysosome compartment.

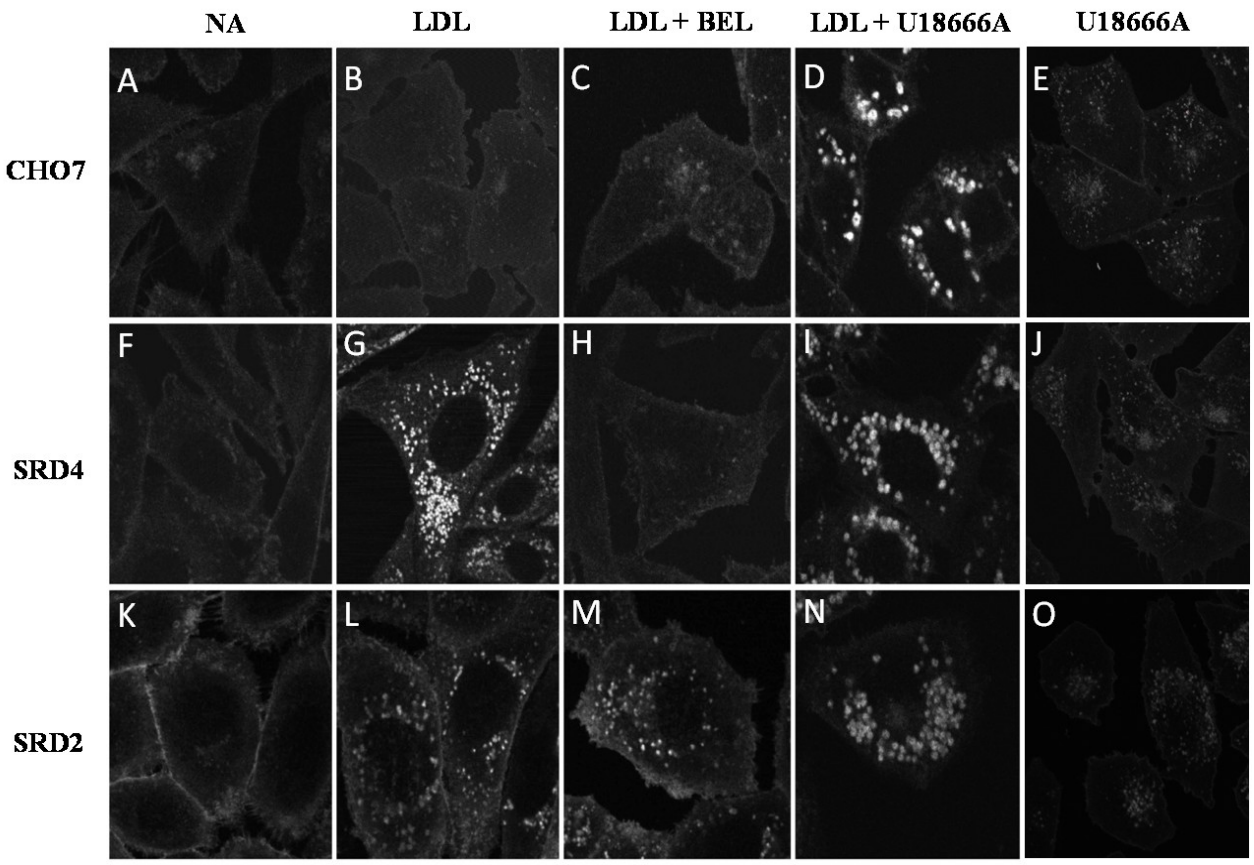

Figure 3.1. Lysosomal free cholesterol accumulation in LDL-treated SRD-4 cells is prevented by the PLA2 inhibitor BEL. CHO7, SRD-2 and SRD-4 cells were plated on coverslips in a 12-well dishes in 1mL of medium B (without supplemental FBS) at a density of 8.0 x 10^4 cells/well on day one. On day two cells were incubated 20 h with no addition (NA) or 50 μg/mL of purified LDL in the absence or presence of 25 μM BEL, before being stained with filipin, which is specific to unesterified cholesterol. In control treatments, cells were incubated with 1 μg/mL U18666A and/or LDL for 20 h to demonstrate LDL uptake in all three cell lines. Magnification is 100X for all images. Representative images are shown, n = 3.

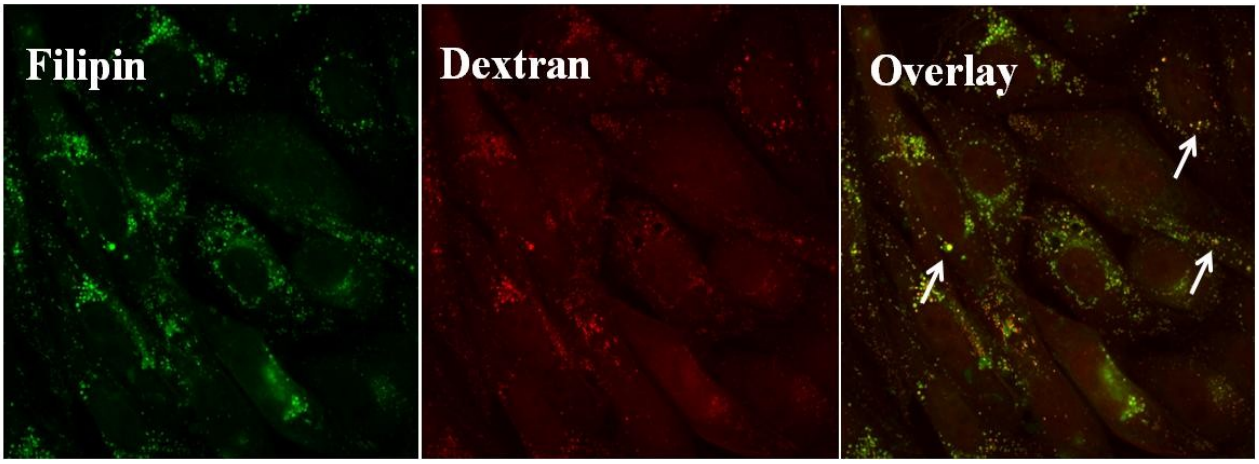

Figure 3.2. Lysosomal accumulation of LDL-derived cholesterol in SRD-4 cells. SRD-4 cells were plated in 12-well dishes in 1mL of medium B (without supplemental FBS) at a density of 8.0 x 10^4 cells/well on day one. On day two SRD-4 cells incubated 20 h with 50 µg/mL LDL and 1 mg/mL Texas Red conjugated Dextran (MW 10,000 kDa) for 1 hour followed by filipin staining. Overlap of Dextran with filipin confirms that the cholesterol build-up is within the lysosomal compartments of SRD-4 cells. Magnification is 100X for all images. Representative images are shown, n=3.

3.1.2 Inhibition of iPLA$_2$ Alleviates Cholesterol Blockage in SRD-4 cells

In addition to defects in the negative feedback control of cholesterol metabolism, SRD-4 cells have also been shown to have increased levels of synthesis and degradation of PC (58). To determine if the increase in PC levels would affect the egress of this blockage of cholesterol within the lysosomes, we employed the use of Bromoenol Lactone (BEL), an irreversible inhibitor of phospholipase A2 (PLA_2),(3) the main enzyme involved in PC degradation in SRD-4 cells (84). We hypothesized that BEL treatment in the SRD-4 cells would allow the naturally occurring increased synthesis of PC to continue, while halting PC catabolism. This should lead to an increase in PC mass. It was shown that treatment of the SRD-4 cells with BEL, in conjunction with LDL, was able to eliminate the lysosomal blockage normally seen with LDL alone (Figure 3.1, panel H). SRD-2 cells were also treated with BEL. The SRD-2 cells have normal PC synthesis and would therefore not have the same increase in PC mass as the SRD-4 cells. In contrast to its effect in SRD-4 cells, BEL did not affect clearance of LDL-derived cholesterol from lysosomes in SRD-2 cells (Figure 3.1, panel M). This work was quantified using the confocal microscope imaging software, and it was shown that the SRD-4 cells indeed return to a more normal level of staining, while the SRD-2 cells maintain their increase (Figure 3.3).

To assess LDL uptake, cell lines were also treated with U18666A; this compound blocks the movement of cholesterol out of the lysosomes, causing cells to accumulate cholesterol in these organelles, much like in cells with NPC1 or NPC2 mutations (63). Treatment of all cell lines with the compound in the presence or absence of LDL showed accumulation similar to that seen in the SRD-2 and SRD-4 cells in the absence of drug treatment (Figure 3.1, panels D, E, I, J, N, and O). This indicated that the parental cell line,

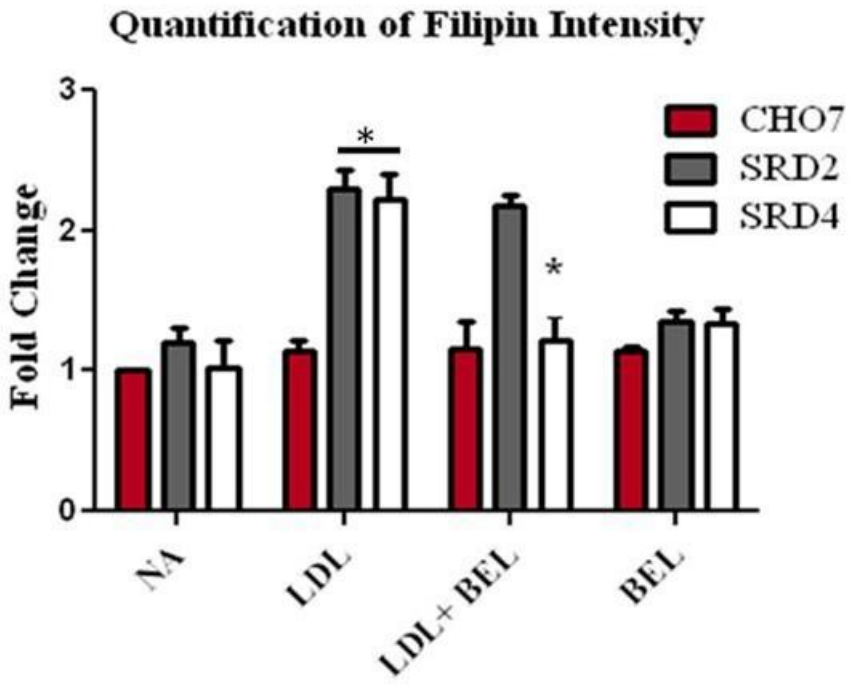

Figure 3.3. Quantification of filipin staining. CHO7, SRD-2 and SRD-4 cells were plated in 12-well dishes in 1mL of medium B (without supplemental FBS) at a density of 8.0 x 10^4 cells/well on day one. On day two cells were treated with 50 µg/mL LDL and/or 25 µM BEL, before being co-stained with filipin and DRAQ5 (DNA binding dye). All BEL treatments were added for 1 hour prior to LDL treatments. Treatments were left on for 20 hours before staining. Filipin intensity in optical sections was quantified using Olympus Fluoview FV1000 software and normalized to total visible cell DNA content for each condition. Values are expressed relative to CHO-7 control cells (no addition – NA), n=3. Error bars represent Standard Error of the Mean. *$p<0.05$ when compared to LDL treatment. N=3.

CHO-7, takes up the LDL in the same manner as the mutant cell lines. Unlike the mutant cell lines, it is able to traffic the LDL-derived cholesterol from the lysosomal compartment.

3.1.3 Analysis of Cellular Cholesterol Content with BEL Treatments

One possibility whereby BEL treatment could prevent lysosomal accumulation of cholesterol is by decreasing LDL uptake and/or total cellular cholesterol levels. As shown in Figure 3.4, total cholesterol content in SRD-4 cells did not decrease with the addition of BEL, but rather increases in all cell lines. This could be due to an increased allowance of cholesterol uptake as a result of the increase in PC. The same can be seen in the treatments with only BEL and may be for the same reasoning. All cell lines have a degree of increased cholesterol content with the addition of the LDL treatment, as expected. Thus the effect of BEL at reversing lysosome cholesterol accumulation in SRD-4 cells is not due to a decrease in LDL uptake or total cholesterol content.

3.1.4 LDLR Protein Analysis under LDL and BEL Conditions

LDLR protein analysis was performed to monitor its levels under the various treatments. It was expected that following treatment with LDL, the LDLR would be down-regulated in accordance with the cholesterol negative feedback pathway in CHO-7 cells but not in the SRD cell lines (Figure 3.5). As expected, LDLR protein levels in CHO-7 cells shows a down regulation with the addition of LDL, as well as with the addition of LDL and BEL (Figure 3.5, lanes 6 and 7 versus 5). This can also be seen to a lesser degree for SRD-4 cells, which was a surprising result as it was expected that the harbored mutations would

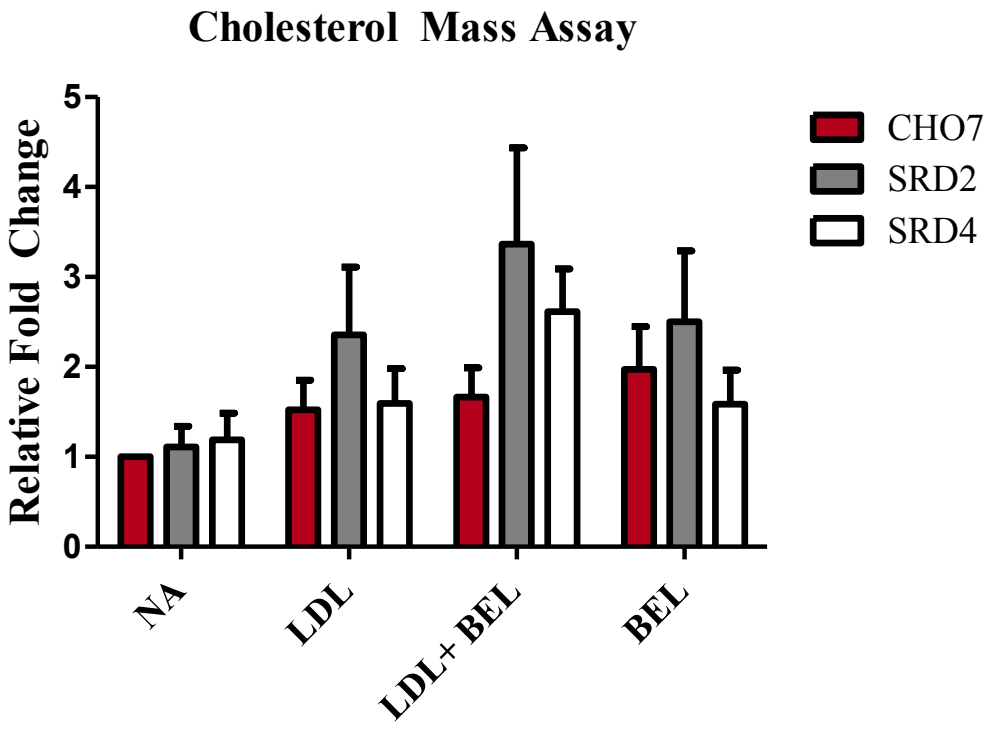

Figure 3.4. Total Cholesterol Mass Analysis. CHO7, SRD-2 and SRD-4 cells were plated in 12-well dishes in 1mL of medium B (without supplemental FBS) at a density of 9.0 x 10^4 cells/well. On day two cells were treated for 20 hours with 50 µg/mL LDL and/or 25 µM BEL, and cholesterol content was analyzed using Cholesterol/ Cholesteryl ester quantification kit (BioVision). BEL treatments were performed for 1 hour prior to addition of LDL for 20 hours, in conjunction with BEL. Values are expressed relative to CHO-7 control cells (no addition – NA), n=5. Error bars represent Standard Error of the Mean.

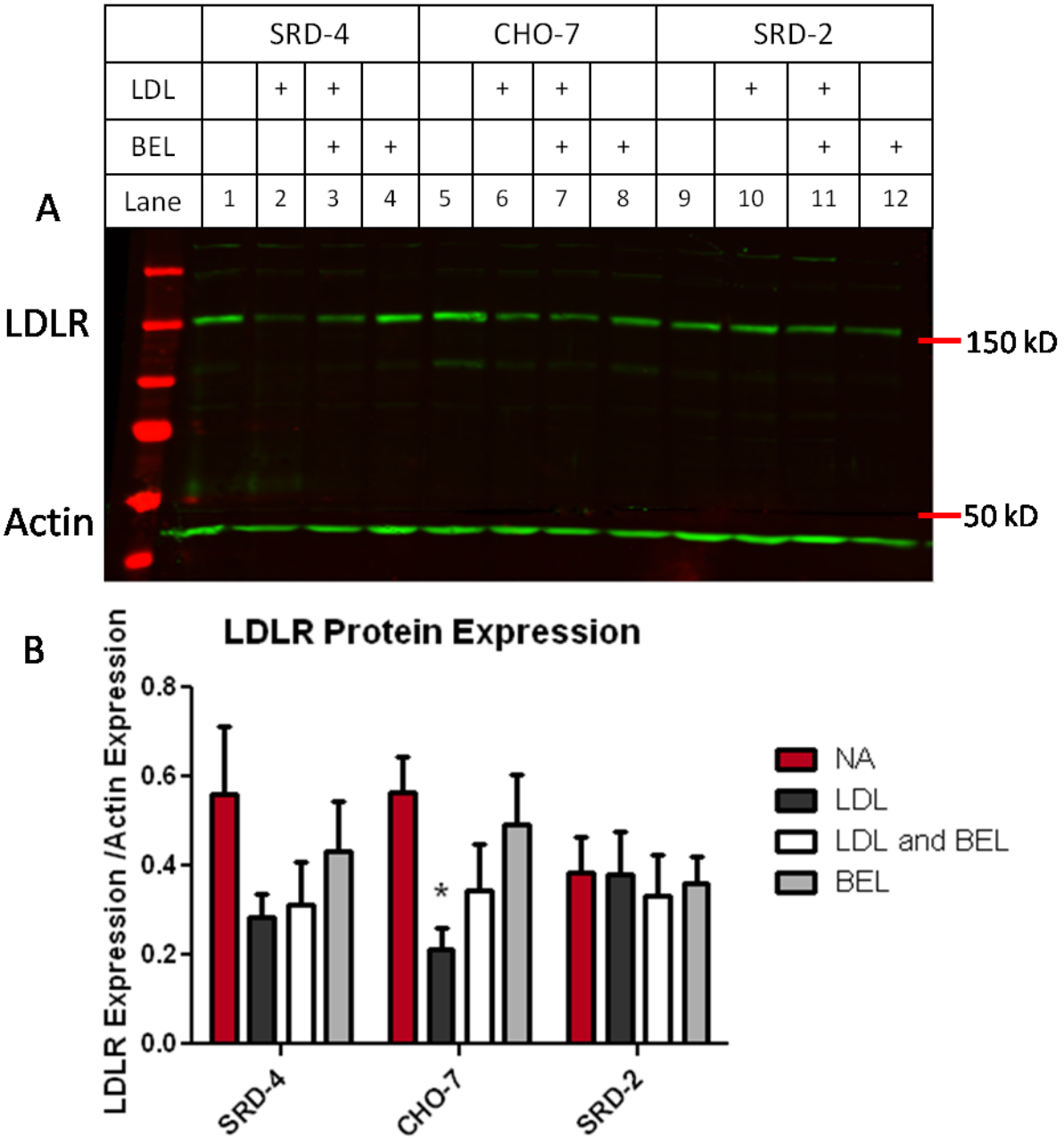

Figure 3.5. LDLR protein expression. CHO7, SRD-2 and SRD-4 cells were plated on 60-mm dishes with 3mL of medium B (without supplemental FBS) at a density of 9.0 x 10^5 cells/well. On day three cells were treated with 50 µg/mL LDL and/or 25 µM BEL for 20 hours. All BEL treatments had a 1 hour pre-incubation. (A) Western blot analysis of LDLR protein content of CHO-7, SRD-2 and SRD-4 cells. (B) Blot is quantified and LDLR expression levels are normalized to actin expression, n=4. Error bars represent Standard Error Mean. *$p<0.05$ when compared to no additions.

cease any regulation of the LDLR (Figure 3.5, lanes 2 and 3 versus 1). While the down regulation is evident, it is not statistically significant ($p = 0.140$). However, it should be noted that the D443N mutation in SCAP in SRD-4 cells does not confer complete resistance to sterols. SRD-2 cells are seen to have almost no regulation of the LDLR receptor, even under high cholesterol conditions, confirming that the truncated SREBP-2 protein does indeed prevent normal regulation (Figure 3.5, lanes 9-12). It is also interesting to note that the SRD-2 cells have lower overall expression levels of LDLR under normal conditions, possibly as an adaptation to compensate for the lack of negative feedback regulation. This result was unexpected and may be a subject for further investigation in the lab.

3.2 Nile Red Staining Reveals Characteristic Lipid Droplet Accumulation

Nile red is a lipophilic dye that preferentially stains intracellular lipid droplets (45, 65). Under basal conditions, the CHO-7 cell lines show very little lipid droplet formation, with an increase when incubated with LDL (Figure 3.6, panel B). The unregulated cholesterol uptake pathway in the SRD-2 cells can account for the appearance of lipid droplets under basal conditions (Figure 3.6, panel C). An extreme increase in the presence of these organelles can be seen following overnight incubation with LDL (Figure 3.6, panel D). In contrast, the SRD-4 cell line lacks functional ACAT and is unable to produce the cholesteryl ester components of lipid droplets, and therefore only had a slight increase in lipid droplet formation after addition of LDL treatment (Figure 3.6, panel E) (70). Despite the ACAT mutation, SRD-4 cells maintain normal triacylglyceride (TG) formation and incorporation, which likely accounts for the slight increase in staining with the addition of LDL (Figure 3.6, panel F) (70). These results indicate that lipid droplets have a large

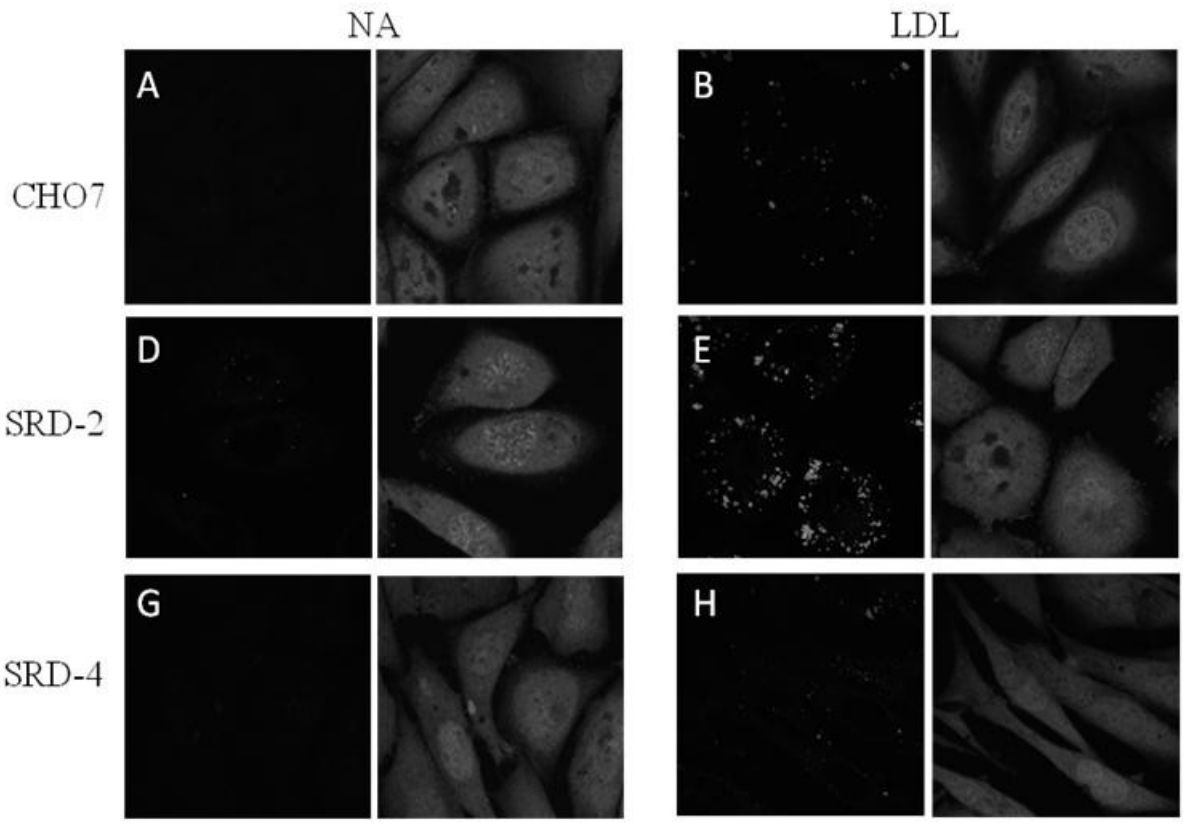

Figure 3.6. Nile red staining reveals characteristic lipid droplet accumulation for each cell type. CHO7, SRD-2 and SRD-4 cells were plated on 12-well plates with 1mL of medium B (without supplemental FBS) at a density of 8.0 x 10^4 cells/well. On day two cells were incubated with 50 µg/mL LDL for 20 hrs and stained with Nile Red and DRAQ5 (5 µM) nucleic acid stain before visualization on the confocal microscope. Nile red stains are seen in the left hand panels, while DRAQ5 is seen in the right hand panels. Magnification is 100X for all representative images. N= 3.

capacity to absorb excess lipid in SRD-2 cells, but not in SRD-4 cells that display the greatest lysosomal accumulation of LDL-derived free cholesterol.

3.3 Methyl-β-Cyclodextrin Overcomes Lysosomal Accumulation in SRD-4 cells

Studies involving mice harboring a knockout of the NPC1 protein have shown that a single injection with the compound cyclodextrin can alleviate the lysosomal blockage caused by the defective transport proteins. This treatment allowed the mice to live longer than their non-treated controls (66). This protection could conceivably be accomplished by the compounds ability to 'trap' hydrophobic molecules within its core and extract them from cells. However, recent evidence suggests that higher concentrations of cyclodextrin are able to enter the cell via endocytosis and work to reduce cholesterol content from within the cell (81). This study by Rosenbaum et al. was able to show that decreased cholesterol content was achieved even after cyclodextrin had been removed from the culture medium, suggesting that the cyclodextrin is working internally.

While the mutations within the SRD-4 cells are different from those of the NPC1 knockout model, the phenotype is comparable. We used a similar compound, Methyl-β-cyclodextrin (CD), on SRD-4 cells treated for 20 hours with 50 μg/mL LDL. 1.5 mM CD was added for 4 hours following this LDL incubation, and the cells were stained with filipin. It was shown that this short incubation with CD was adequate to clear the SRD-4 cells of the lysosomal blockage (Figure 3.7). A control was performed where the LDL was removed from the cells and no CD was added for the chase period. This was to confirm that this time period would not be sufficient for the cells to clear the cholesterol themselves. This finding

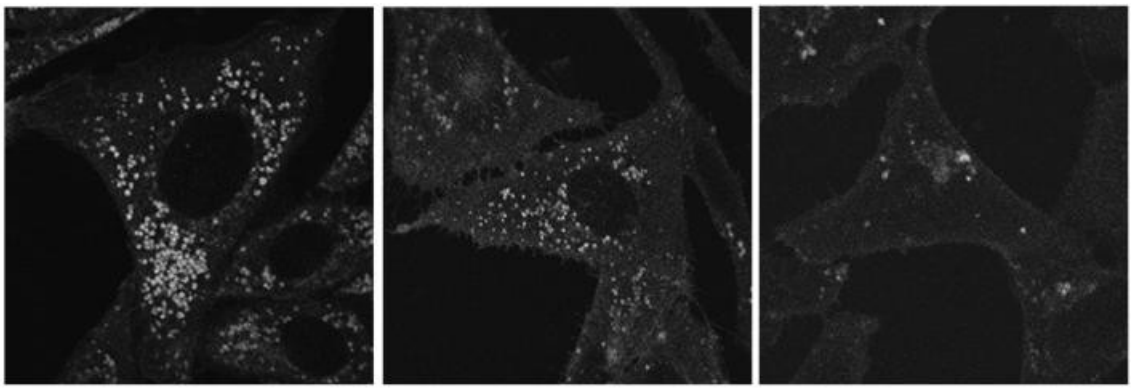

Figure 3.7. Lysosomal build-up in LDL-treated SRD4 cells is due to overall cellular cholesterol loading. SRD-4 cells were plated on 12-well dishes with 1mL of medium B (without supplemental FBS) at a density of 8.0 x 10^4 cells/well. On day two SRD-4 cells were incubated 20 h with 50 μg/mL of purified LDL. After 20 hours of incubation, LDL was removed, and cells were incubated in medium B containing 1.5 mM Methyl β-cyclodextrin (CD) to extract free cholesterol or no addition (NA) for a 4 h chase period prior to fixation and filipin staining. Magnification is 100X for all representative images. N=3.

suggests that the lysosomal build-up in LDL-treated SRD-4 cells is due to overall cellular cholesterol loading.

3.4 Lyso-PC and Propranolol have Reverse Effects on Cholesterol Accumulation

3.4.1 Lyso-PC Alleviates Cholesterol Blockage in SRD-2 and SRD-4 cell lines

The CDP-choline pathway is responsible for the synthesis of PC, using choline and fatty acids as precursors. It is also possible to reacylate lyso-PC, the product of the enzymatic action of $iPLA_2$, to create PC. This process is accomplished by a lysophospholipid acyltransferase, which has the ability to use a fatty acid chain in conjunction with lyso-PC to create PC (76). We considered the possibility that alleviation of cholesterol accumulation was possible by feeding the pathway the necessary compounds to make PC. By using lyso-PC, we have shown alleviation of a large portion of the lysosomal blockage seen in SRD-2 and SRD-4 cells (Figure 3.8). This was accomplished with a 20 hour co-incubation of 50 μg/mL LDL and 50 μM lyso-PC, followed by filipin staining. This mirrors previous experiments in which we used BEL to inhibit $iPLA_2$, the enzyme used to breakdown PC formed endogenously. In both cases, providing the cells with a means to increase cellular PC has allowed alleviation of the cholesterol blockage seen in SRD-2 and SRD-4 cell lines (Figure 3.8).

3.4.2 Propranolol Induces a Cholesterol Blockage in CHO-7 cell line

We next sought to determine the effects on cholesterol trafficking of limiting the cells ability to create PC, in contrast to the experiments where cellular PC was increased. R-Propranolol (Prop) is a compound that inhibits phosphatidic acid phosphatase (PAP) (74).

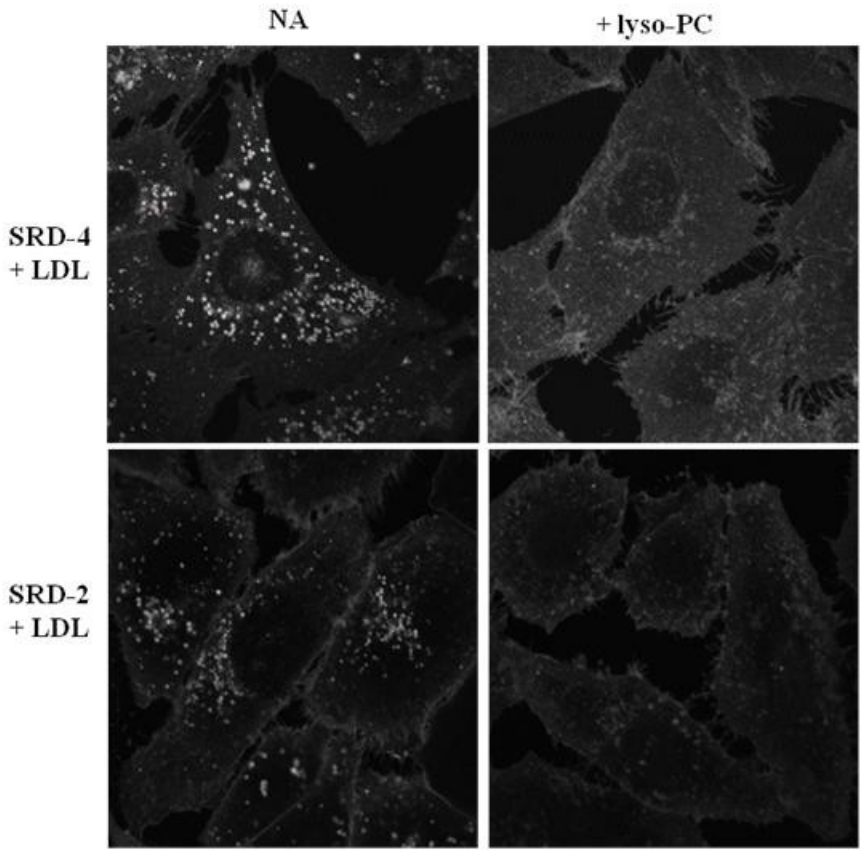

Figure 3.8. Lysosomal free cholesterol accumulation in LDL-treated SRD-4 and SRD-2 cells is prevented by supplementation with Lyso-PC. SRD-4 and SRD-2 cells were plated in 12-well plates with 1mL of medium B (without supplemental FBS) at a density of 8.0 x 10^4 cells/well. On day two cells were incubated for 20 h with 50 μg/mL of purified LDL in the absence or presence of 50 μM lyso-PC, prior to fixation and filipin staining. Representative fields are shown. Magnification is 100X for all representative images, n = 3.

This action would in turn attenuate the production of diacylglycerol (DAG), a needed substrate in the synthesis of PC from its precursor CDP-choline (Figure 1.5). The treatment of the CHO-7 cells, which harbor no cholesterol pathway mutations, with LDL and Prop, created a lysosomal cholesterol accumulation similar to that seen in the cholesterol defective SRD-2 and SRD-4 cells treated with LDL (Figure 3.9, panel A). Treatment of these mutant SRD cells with both LDL and Prop further increased the degree of cholesterol accumulation (Figure 3.9, B and C). All cells generally tended to take up less surface area with the Prop treatment, resulting in an inability to quantify of images using the same techniques employed previously. In all three cases, easing of this blockage was achieved with an overnight co-treatment with lyso-PC (Figure 3.9, D-F), supporting that either lyso-PC or PC was facilitating cholesterol movement. Complete alleviation was not achieved; this could perhaps be attributed to other effects of Prop on the cells.

3.4.3 Propranolol Decreases the Synthesis of PC

Propranolol has been shown to work by inhibiting PAP; this would in turn affect the output of newly synthesized PC by reducing the cellular DAG pool. We sought to confirm the mechanism of action of Prop with metabolic studies using radiolabeled choline ([^{3}H] Choline). By monitoring the CDP-choline pathway via the incorporation of this labeled choline, we were able to determine the specific effects of Prop on the pathway. Data showed that with LDL and Prop treatments, there was a 47% and 62% decrease in PC synthesis in SRD-2 and CHO-7 cell lines, respectively, when compared to LDL treatments ($p < 0.001$) alone (Figure 3.10, panel A). This indicated that Prop had a negative effect on the synthesis of PC. Choline levels were also monitored in the same experiment to ensure

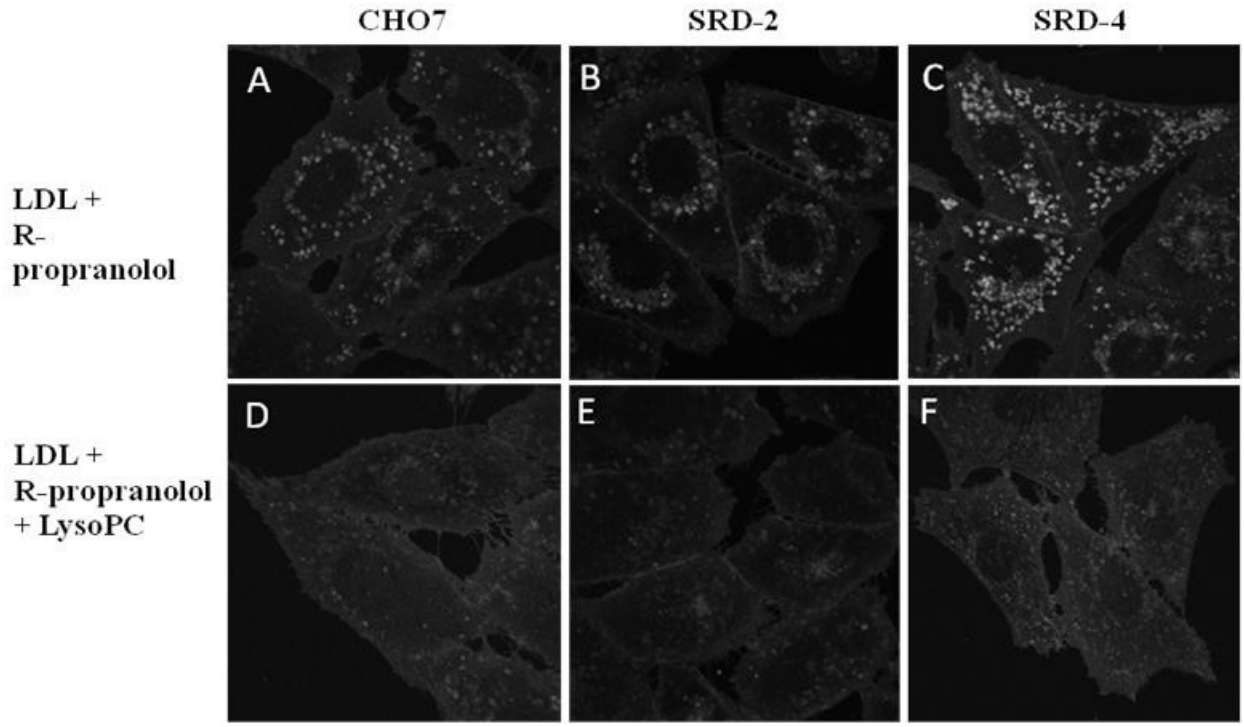

Figure 3.9. Lysosomal accumulation of LDL-derived cholesterol is induced by the phosphatidic acid phosphatase (PAP) inhibitor Propranolol and partially relieved by Lyso-PC. CHO7, SRD-2 and SRD-4 cells were plated on 12-well plates with 1mL of medium B (without supplemental FBS) at a density of 8.0 x 10^4 cells/well. On day two cells were incubated for 20 h with 50 μg/mL of purified LDL in the presence of 60 μM R-Propranolol and 50 μM lyso-PC; cells were then stained with Filipin. All representative images were acquired at 100X magnification, n=3.

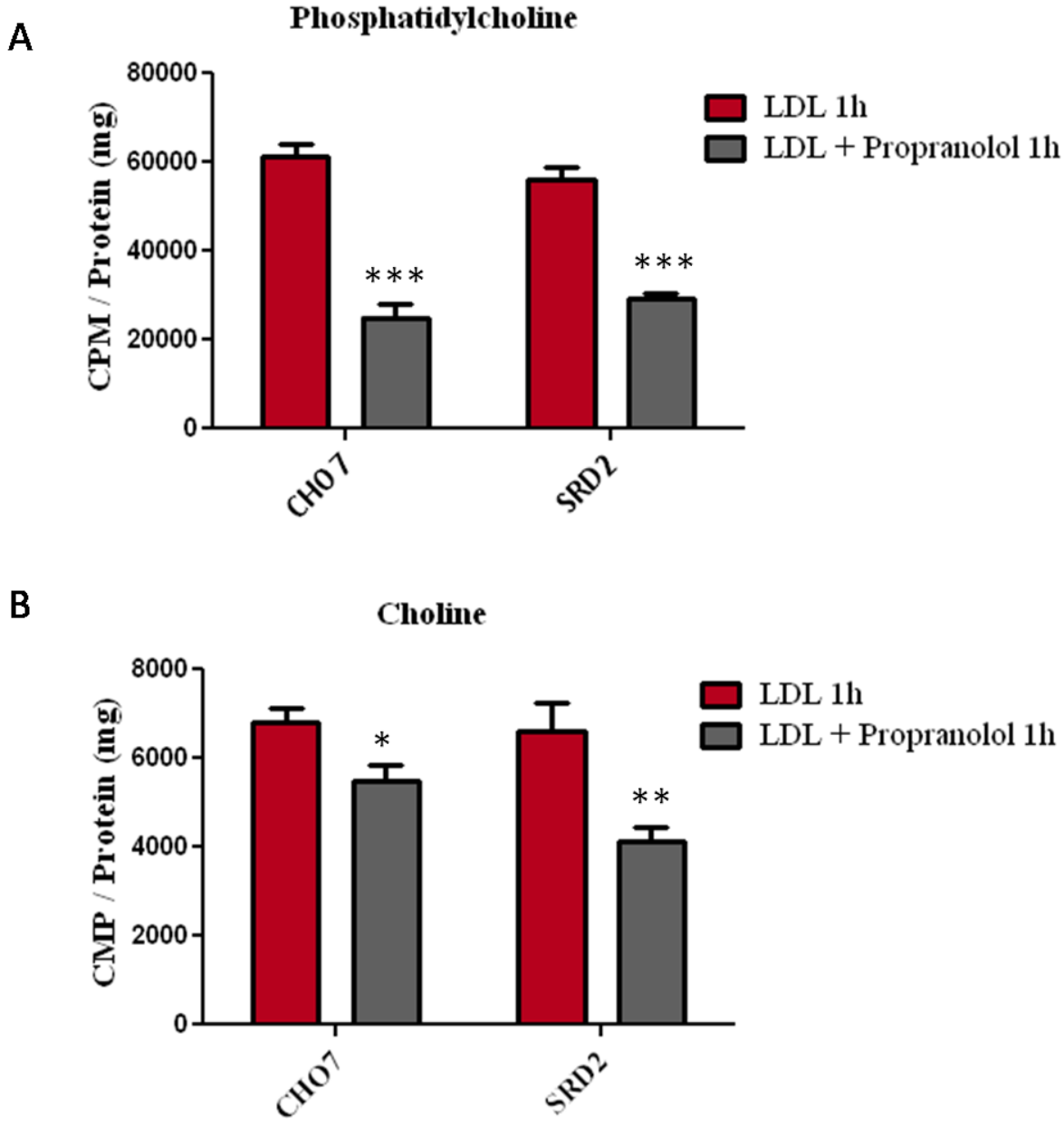

Figure 3.10. Propranolol decreased phosphatidylcholine production in CHO-7 and SRD-2 cells. CHO7, and SRD-2 cells were plated on 60-mm dishes with 3mL of medium B (without supplemental FBS) at a density of 9.0 x 10^5 cells/dish. On day two cells were treated with 50 µg/mL LDL and/or 60 µM propranolol for 1 hour prior to 1 hour incubation with 6 µCi ^{3}H labeled choline. Lipid extracts were then analyzed for several of the CDP-choline pathway metabolites. (A) Phosphatidylcholine synthesis is analyzed. (B) Choline levels are analyzed. Error bars represent Standard Error of the Mean. *$p<0.05$ when compared to LDL treatment. **$p<0.005$ when compared to no LDL treatment. ***$p<0.001$ when compared to LDL treatment, n=3.

that decrease in choline levels was not responsible for the decrease in PC synthesis (Figure 3.10, panel B). Our data indicate that the decrease in choline uptake is significant in both cell lines with the treatment with Prop (20%; $p < 0.05$ for CHO-7 cells and 37%; $p < 0.005$ for SRD-2 cells, when compared to LDL treatments alone); however, the magnitude of the decrease in PC synthesis following treatment with Prop is significantly larger. This leads us to believe that the decrease in choline levels do not account for the decreased PC synthesis in CHO-7 and SRD-2 cells and that Prop is indeed working by reducing the synthesis of PC. Due to the altered CDP-choline pathway in SRD-4 cells this method of analysis proved inconclusive, and often confusing. For this reason we opted to eliminate the SRD-4 cell line from further analysis.

3.5 All Cell lines contain NPC1 Protein

While the SRD cell lines contain mutations that disable their ability to properly regulate the uptake and synthesis of cholesterol, it was assumed that their NPC1 protein function was normal. This would mean that the mechanism of cholesterol release could be achieved via the NPC hand-off model that is seen in normal cholesterol movement scenarios. It has also been shown that NPC1 contains an SRE element and can therefore be regulated via the SREBP pathway (36). To confirm this, we performed western blotting techniques on non-treated cells. It can be seen that all three cell lines contain the NPC1 protein (Figure 3.11). Interestingly, the SRD-2 cell line expresses the highest levels ($p < 0.001$, compared to the CHO-7 cell line), with SRD-4 expressing approximately 33% less ($p < 0.05$, compared to the CHO-7 cell line). The CHO-7 cell line shows the lowest expression levels, roughly 66% less than that of the SRD-2 cells. Using immunofluorescence

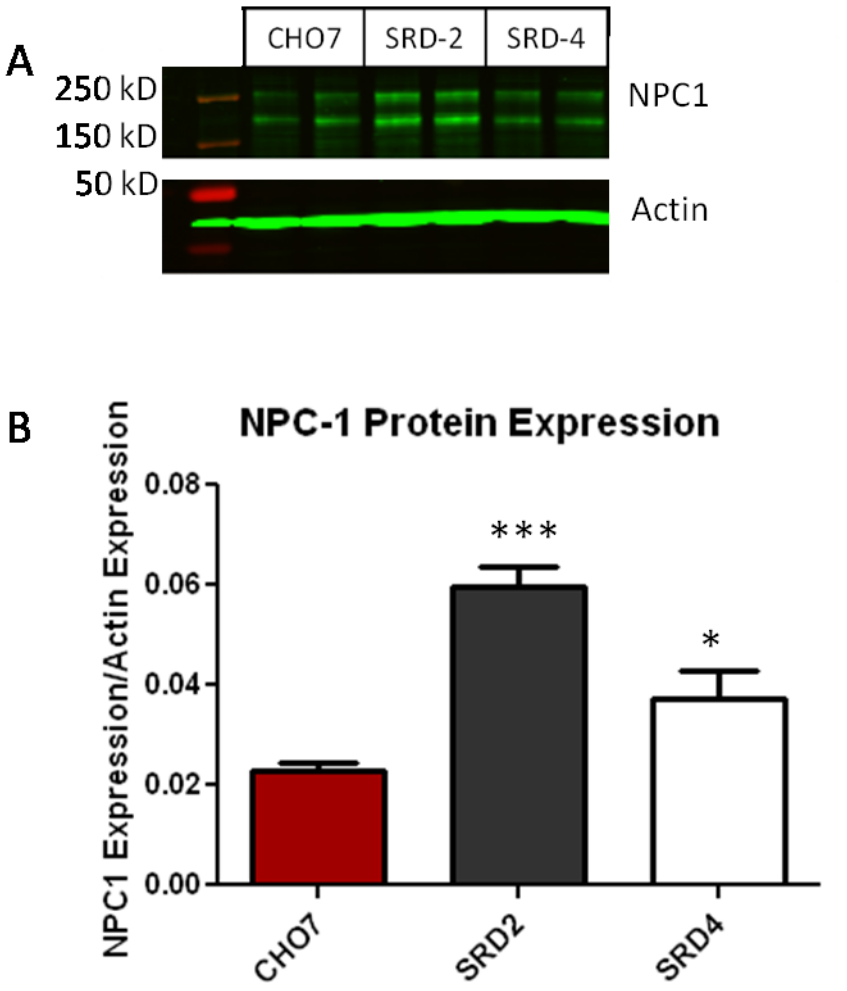

Figure 3.11. NPC1 protein expression levels. CHO7, SRD-2 and SRD-4 cells were plated on 60-mm dishes with 3mL of medium B (without supplemental FBS) at a density of 9.0 x 10^5 cells/dish. On day two cells were collected and lysed for protein content analysis. (A) Western blot analysis of NPC1 protein content of CHO-7, SRD-2 and SRD-4 under normal conditions. (B) Western blot was quantified and expression levels were normalized to actin expression, n=2. Error bars represent Standard Error of the Mean. *$p<0.05$ when compared to CHO-7 cells. ***$p<0.001$ when compared to CHO7 cells.

techniques, we looked at both endogenous levels of NPC1, as well as those induced by LDL and Prop treatments. Basal levels mirrored what was seen with western blot analysis. SRD-2 cells showed the greatest levels of NPC1 protein under all conditions, with SRD-4 and CHO-7 cells showing very little (Figure 3.12, panels A-C). SRD-4 cells showed an increase with LDL treatment, as well as LDL and Prop treatment (Figure 3.12, panels F and I). CHO-7 cells showed detectable NPC-1 protein only with LDL and Prop treatment (Figure 3.12, panel G).

3.6 Flow Cytometry Confirms that Treatments do not Prevent Uptake of LDL

To ensure that the treatments used were not impairing the uptake of LDL into the cells, we applied flow cytometry techniques to all cell lines and treatments. Cells were treated with 1.5 μg/mL of Dil-labeled LDL (Dil-LDL) in conjunction with each of the treatments used in all previous experiments. This was compared to Dil-LDL uptake during non-treatment conditions. It was determined that the treatments used did not impair LDL uptake in any notable manner. As a control to show that the uptake seen was specific, we used 300 μg/mL non-labeled native LDL with the standard 1.5 μg/mL Dil-LDL treatment. This non-labeled LDL was able to compete off the Dil-LDL, showing greater than 75% specificity (Figure 3.13).

3.7 ACAT Washout Timeline

SRD-4 cells harbor a mutation within an allele for ACAT, rendering the enzyme inactive.(20) The ACAT inhibitor 58-035 has been used for several decades as a specific inhibitor of ACAT activity (82). Since cholesterol accumulation was greater in the SRD-4

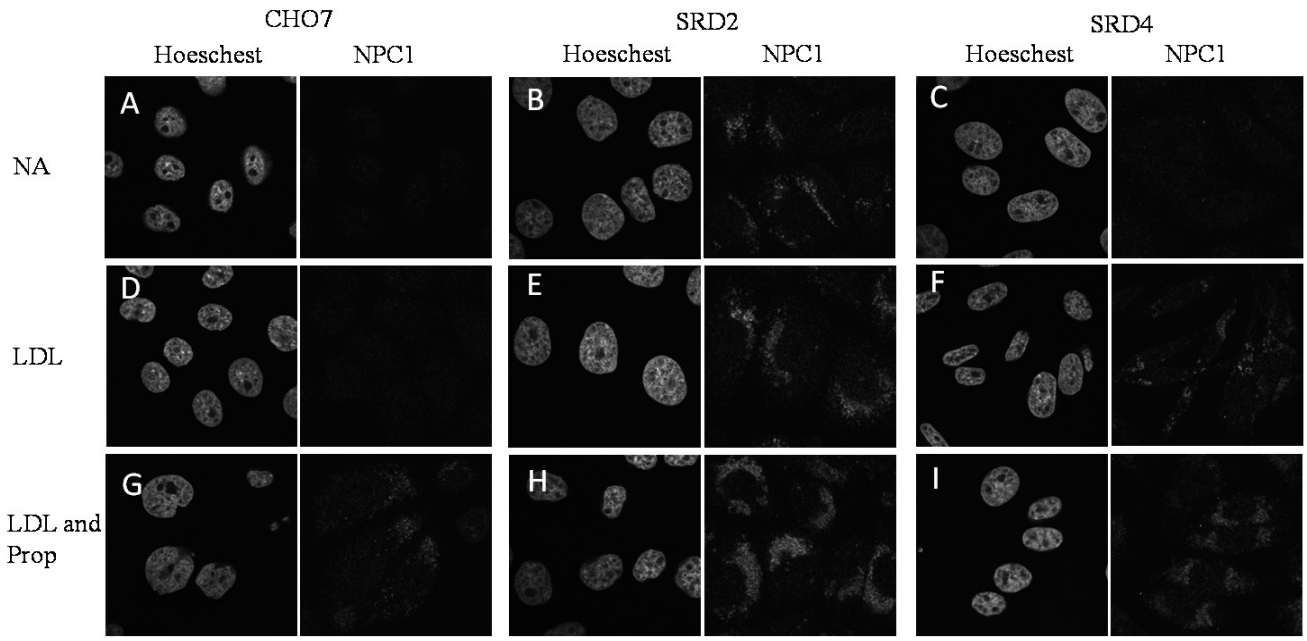

Figure 3.12. Immunoflourescence of NPC1. CHO7, SRD-2 and SRD-4 cells were plated on 12-well plates with 1mL of medium B (without supplemental FBS) at a density of 8.0 x 10^4 cells/well. On day two cellular NPC1 levels were examined in all cell lines using immunofluorescence techniques. Cells were incubated with no additions, 50 µg/mL LDL and/or 60 µM propranolol for 20 hours before staining. Cells were also stained with Hoeschest (2µg/mL), a nuclear dye. All representative images were acquired at 100X magnification, n=2.

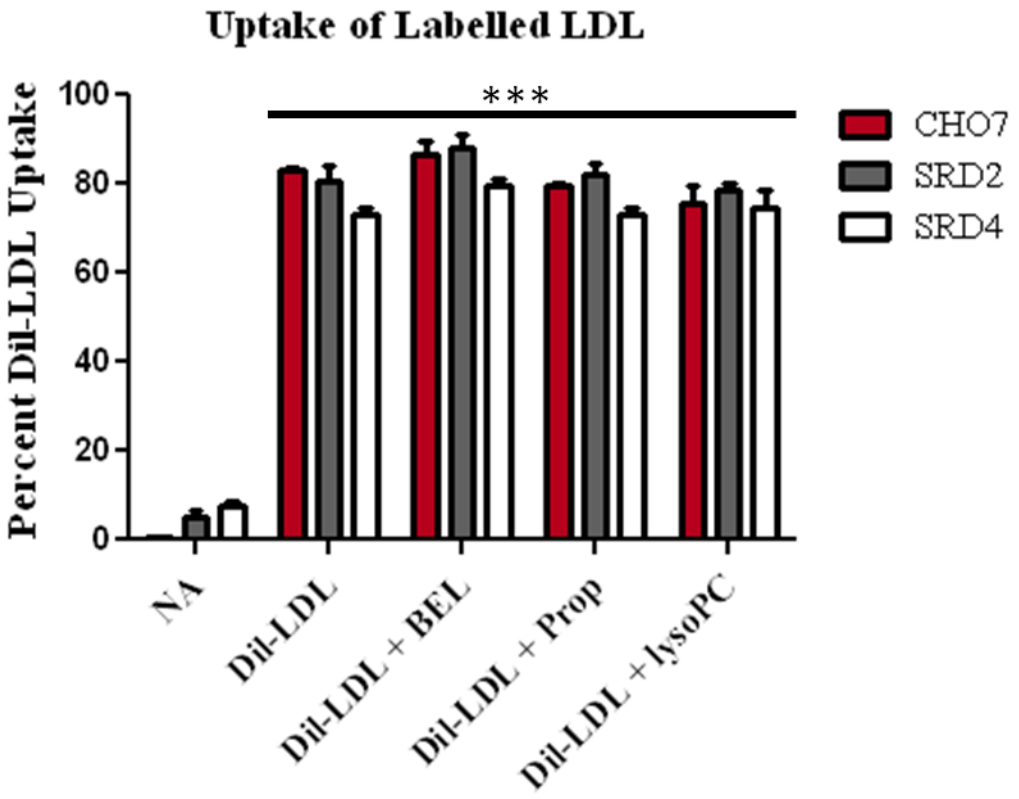

Figure 3.13. Relative LDL uptake in cell lines incubated with various treatments. CHO7, SRD-2 and SRD-4 cells were plated on 12-well plates with 1mL of medium B (without supplemental FBS) at a density of 3.0 x 10^5 cells/well. On day two cells were incubated the various treatments as stated previously, with the addition of 1.5 µg/mL of DiI-labeled LDL for 3 hours before collection and analysis via Flow Cytometry. This treatment was used to quantify the relative LDL uptake under each condition. Dil-LDL was competed with 300 µg/mL unlabelled LDL to show >75% specificity of the binding and uptake. Error bars represent Standard Error of the Mean. ***$p<0.001$ when compared to no additions, n=3.

cells, which lack ACAT activity, the role of this enzyme in the movement of LDL-derived free cholesterol from lysosomes was investigated in SRD-2 cells using the ACAT inhibitor. SRD-2 cells treated with the LDL in conjunction with 58-035 are seen to accumulate a notably larger amount of lysosomal cholesterol compared to LDL alone (Figure 3.14, panel G). A slight increase is seen in the SRD-4 cells under the same conditions, however since these cells do not have ACAT activity no remarkable change was expected (Figure 3.14, panel L). The parent cell line CHO-7 did not show any phenotypic change with these treatments, as the cell line contains the machinery necessary to properly regulate LDL uptake when ACAT is not active (Figure 3.14, panels A-E).

A washout of the 58-035 was performed to determine if resumption of ACAT activity would facilitate the movement of cholesterol out of the lysosomes. Over an eight hour time course a decrease in lysosomal blockage is seen in the SRD-2 cells (Figure 3.14, panels H-J versus G). The same can be seen in the SRD-4 cells although to a lesser extent (Figure 3.14, panels M-O versus L). The reason for lysosomal cholesterol depletion over time in ACAT-deficient SRD-4 cells is unclear, but could involve ACAT-independent mechanisms, for instance cholesterol removal from the cell via acceptors in the medium or membrane shedding.

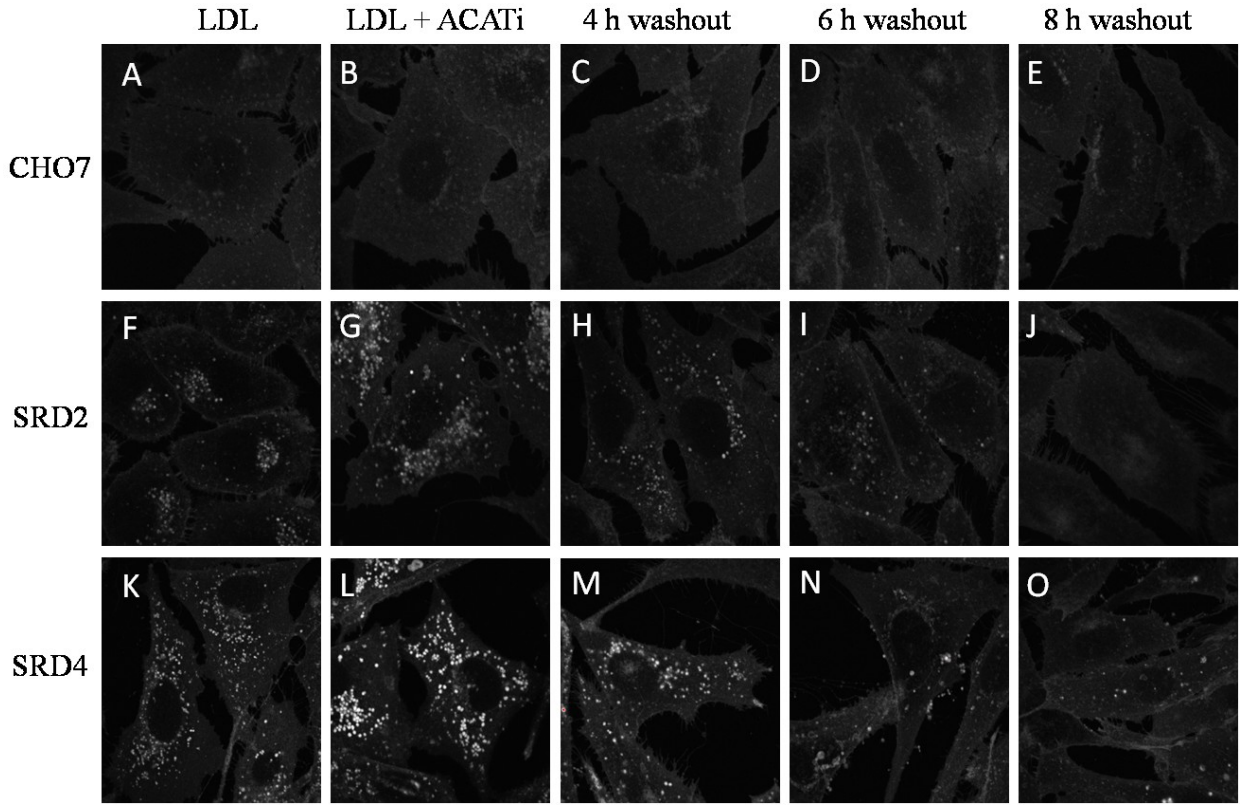

Figure 3.14. ACAT inhibitor (58-035) washout timeline. CHO7, SRD-2 and SRD-4 cells were plated on 12-well plates with 1mL of medium B (without supplemental FBS) at a density of 8.0 x 10^4 cells/well. On day two cells were incubated with 50 µg/mL of LDL as well as 2.5 µg/mL of the ACAT inhibitor 58-035 for 20 hours. Cells were washed for the indicated time, stained with filipin and analyzed by confocal microscopy. All representative images were acquired at 100X magnification, n=2.

4 Discussion

Cholesterol overloading or depletion conditions are highly detrimental to the cell. The regulation of cholesterol movement, synthesis and uptake is therefore well regulated (13). Our work has focused on the role of PC in the egress of LDL-derived cholesterol out of the lysosomal compartments. PC is the most abundant phospholipid within the cell and plays a significant role in many cellular pathways (29). The ratio of cholesterol to PC is highly defined with little range for adjustment (92). Our hypothesis states that the ratio of PC to free cholesterol in downstream organelle membranes can influence the movement of cholesterol out of lysosomal compartments in cholesterol-loaded cells.

4.1 Lysosomal Cholesterol Loading as a Protective Mechanism

Sterol regulatory (SRD) cell lines used in this work allowed for a visual appreciation of the effects of cholesterol dysregulation on the cell. Normal cell lines under cholesterol rich conditions are able to turn off cholesterol uptake machinery, such as the LDLR, and properly regulate the movement of cholesterol within the cell (16). In the case of the SRD-2 and SRD-4 cells, the impaired cholesterol sensing pathways lead to continual LDL uptake and resultant lysosomal accumulation of unesterified cholesterol (Figures 3.1 and 3.2). Parental CHO-7 cells, used throughout this study as a control, show no lysosomal loading effects of this same LDL treatment. The effects of LDL loading on the SRD-2 and SRD-4 cell lines resemble the phenotype seen in NPC1 defective cells. SRD-2 and SRD-4 cells lose the ability to traffic cholesterol out of the lysosomes due to their mutations. While the SRD cell lines maintain NPC1 function (Figure 3.11), they are unable to properly traffic the unnaturally high amount of cholesterol taken up.

It seems likely that the inability to traffic cholesterol in LDL-treated SRD cells is due to cholesterol accumulation in downstream membranes and an inability of these membranes to accommodate more cholesterol molecules, creating a 'bottle-neck' effect. Cholesterol accumulation within the lyososmal compartments has also been suggested to be induced in cells as a protective mechanism during cholesterol loading (91). This would isolate the excess cholesterol and shield the cell from the detrimental effects of cholesterol overloading, which include cholesterol crystallization, ER stress, and the induction of apoptosis. Evidence for this theory comes from a wide variety of sources (93, 94).

NPC1 is not obviously regulated by the SREBP pathway in the manner that LDLR is known to be. Until recently, its role in the regulation of cholesterol homeostasis was unknown. Recent work has shown striking evidence for the down regulation of both the NPC1 and NPC2 proteins during LDL loading conditions (34, 51). Interestingly enough, this is not the first report of NPC down regulation due to cholesterol overloading. Cells with heterozygous NPC1 expression have previously been shown to have increased levels of LDL-derived cholesterol within 'undefined endocytic compartments' as well as impaired movement of cholesterol to the trans-Golgi network (35, 56). These studies provide examples of conditions where impaired NPC1 function, either via genetic or physiological means, leads to a similar biochemical fingerprint, resulting in the sequestration of LDL-derived cholesterol. These studies mirror the known regulation of the SREBP pathways, including the down regulation of Insig-1 and SCAP, in addition to the presented evidence for NPC-1 regulation (14, 83). This also highlights a mechanism employed by the cell to sequester LDL-derived cholesterol within the lysosomes, possibly as a protective measure.

This leads to our interpretation that the lysosomal accumulation in the SRD-2 and SRD-4 cells is protective. The SRD-4 cells show a greater degree of accumulation due to their impaired ACAT function (Figure 3.1), while the SRD-2 cells show a robust accumulation of lipid droplets under the same conditions (Figure 3.6). Taken together, this phenotype would suggest that cells employ a protective mechanism to prevent cholesterol overloading and the subsequent toxic effects. Our data indicates that NPC1 protein is expressed (Figure 3.11) and properly localized to lysosomes (Figure 3.12) in SRD cells, thus impaired NPC1 function cannot account for defects in lysosomal cholesterol trafficking seen in the SRD cell lines, and other mechanisms must be considered.

4.2 Increasing Cellular Levels of PC allows Cholesterol Movement

It has been shown that the accumulation of cholesterol is concurrent with cellular increases in PC levels in a multitude of cell types (58, 86, 93). These reports, and others, have hypothesized that this represents an adaptive mechanism adopted by the cell to adjust to the large cholesterol imbalance that occurs during unregulated uptake (92, 94). This would effectively help to return the PC to free cholesterol ratio to a more manageable level. In terms of lysosomal cholesterol accumulation as a protective mechanism, this could allow the egress of cholesterol from within the lysosomal compartments without cholesterol toxicity occurring. Our data support this hypothesis. SRD-4 cells are known to harbor disrupted pathways causing an increase in PC synthesis. Interestingly, these cells are able to recognize the harm in constant excess PC and have a similar increase in PC catabolism (58). This causes the overall mass of the PC in the SRD-4 cells to remain similar to its parental cell line, despite the changes in pathways. By using the $iPLA_2$ enzyme inhibitor BEL, the

degradation of PC into lyso-PC within the cell would be halted (3). In the case of the SRD-4 cells this would result in an increase in PC mass. Using this compound with an LDL treatment resulted in greatly reduced lysosomal cholesterol buildup compared to the LDL treatment alone (Figure 3.1). This was not the case for the SRD-2 cells, where the lysosomal cholesterol loading persisted. These cells do not contain the increased activity of the CDP-choline pathway as the SRD-4 cells do. This leads us to suggest that it is an increase in PC mass in the SRD-4 cells that allows the lysosomal cholesterol loading to be abolished. Using whole-cell PC mass assays (lipid phosphorus), we were unable to show a significant increase in PC mass in SRD-4 cells treated with BEL (data not shown). It is possible that increased PC levels may occur in specific membranes or at low enough levels as to not greatly affect overall cellular PC mass. It is also important to note that BEL has known effects on the activity of PAP, which would in turn effects the output of DAG. This would compromise the ability of the cell to synthesize PC from CDP-choline. We anticipate that the effects on PC degradation are greater than that on the DAG depletion; however this remains to be determined. A knockdown of $iPLA_2$ would confirm whether PC degradation plays a role in lysosomal cholesterol sequestration. Future experiments could also examine changes in PC-to-cholesterol ratios in specific membranes, such as ER membranes, using subcellular fractionation methods.

Cholesterol mass assays were performed on cell lines treated with LDL and BEL to determine if the BEL treatment was inhibiting cholesterol uptake rather than facilitating cholesterol trafficking (Figure 3.4). Interestingly, the LDL and BEL treatments compared to the LDL alone saw more cellular cholesterol mass in all three cell lines. This could be due to the increased PC allowing the cells to take up more cholesterol, while allowing the PC-to-

cholesterol ratio to remain at a normal level. Even in conditions with no LDL, the BEL treatment caused an increase in cholesterol, suggesting that the cells are endogenously making more cholesterol to balance out the increase in PC. However, this conclusion would require further investigation on the effects of increased PC levels on cholesterol synthesis. As is the case for most inhibitor studies, we cannot rule out that BEL could be exerting non-specific effects on metabolism in these cells independent of its known effect on PLA_2 activity.

Western blot analysis of the LDLR for all three cell lines under the BEL and the LDL conditions had surprising results (Figure 3.5). CHO-7 cells showed the appropriate down regulation of the LDLR upon LDL treatment. Both the SRD-2 and SRD-4 cell lines harbor mutations causing their cholesterol regulatory pathways to be defective (20, 70, 99). For this reason, we anticipated that both cell lines would have no regulatory response to the LDL treatments. While this was true of the SRD-2 cells, the SRD-4 cells mirrored the response of the CHO-7 cells, with down regulation of the LDLR due to LDL treatments. This leads us to believe that the SRD-4 cells have adopted an altered regulatory method to avoid constant LDLR expression under critical conditions. A recently discovered E3 ubiquitin ligase, known as IDOL (inducible degrader of LDLR), has been shown to have transcriptional up-regulated via LXR. This ligase causes the internal degradation of LDLR during cholesterol rich conditions (101). It would be interesting to examine the levels of IDOL within all cell types as a possible explanation for the confounding LDLR expression levels. It is also interesting to note that the SRD-2 cells have an overall lower expression of this receptor, possibly as an adaptation to prolonged cholesterol uptake. We saw that under LDL loading conditions the SRD-2 cells had incredibly enlarged lipid droplets (Figure 3.6),

which are presumably able to balance out some of the cholesterol overloading. The SRD-4 cells do not have this reservoir option as they do not contain functional ACAT (20). This could explain the unexpected LDLR down regulation in SRD-4 cells and the need for an alternate adaptive mechanism.

Additionally, genetic studies could be applied to these results. The decrease in cholesterol loading suggests that free cholesterol egress from lysosomes could increase negative feedback control of SREBP processing. RT-PCR analysis of SREBP target genes under these conditions would further highlight the hypothesis that the BEL treatment and cholesterol movement is affecting these pathways, whereas before there was a 'bottle neck' effect preventing overall cholesterol levels within the cells from being sensed by the SREBP pathway protein machinery in the ER.

In a more striking result, we were able to clear lysosomal accumulation of LDL-derived cholesterol in both the SRD-2 and SRD-4 cells with the use of lyso-PC (Figure 3.8). This compound can be reacylated to create PC once in the cell via the Lands pathway. This corroborates the data gathered with the treatment of the cell lines with BEL. Rather than inhibiting the degradation of PC, we supplied the cell with the means to increase their PC content and overcome the cholesterol blockage. As we were not able to definitely prove that the lyso-PC was reacylated to PC using ^{3}H-labeled lyso-PC (data not shown) more research into this area is needed. We cannot exclude the possibility that the lyso-PC is acting in a separate manner all together, perhaps from outside the cell, or that the fatty acid chains of the lyso-PC are being used in a signaling cascade. A study using mouse peritoneal macrophages showed that lyso-PC enhanced the efflux of cholesterol from lipid laden foam cells created by cholesterol loading (45a). This group was able to show that with this efflux

paralleled an increase in the expression of apoE. Therefore, it is possible that the effects of lyso-PC are, for example, due to the stimulation of a signaling cascade that results in the synthesis of efflux machinery.

Attempting to draw a parallel to the results seen with lysosomal storage disorder cells we used a compound shown to reverse NPC disease in cyclodextrin. When used on SRD-4 cells methyl β-cyclodextrin (CD), was able to parallel the results seen in previous studies in which cells and mice harboring NPC mutations were relieved of cholesterol loading with treatments (1). Use of CD for a short period of time was able to relieve cells of the cholesterol blockage that had been loaded with LDL for 20 hours. This was not enough time for the cells to accomplish this feat on their own, as seen by controls (Figure 3.7). Several models of extraction have been argued. One argument is that using CD in low concentrations, as we have here, can work by extracting cholesterol from the plasma membrane. This would, hypothetically, cause the cholesterol accumulation within the lysosomes to be alleviated due to the decreased overall cellular cholesterol, returning the PC to cholesterol ratio of the cell to a more acceptable level. A second potential mechanism involves the uptake of CD into the lysosomes, where it will interact with NPC2. It has also been shown that CD has the potential to deliver the cholesterol laden lysosomes to the plasma membrane for exocytosis from the cell (68, 81).

NPC1 protein expression was examined in the SRD and CHO-7 cell lines to ensure that the cholesterol had the means to be exported from the lysosomes in a normal manner. SRD-2 cells had the highest overall basal expression levels, possibly as another adapted method to attempt to control the constant cholesterol overloading. SRD-4 cells also showed higher levels of NPC1 expression than that of the CHO-7 cells, possibly for the same

reasons (Figure 3.11). NPC1 expression levels during immunofluorescence studies showed an increase in both the SRD-2 and SRD-4 cells with the addition of LDL, while CHO-7 cells maintained a more basal level of the NPC1 protein expression regardless of LDL treatment (Figure 3.12). This suggests that while the SRD cell lines have the means to export the cholesterol from their lysosomes, it is instead maintained in these compartments to protect the cell.

4.3 Inhibiting the Synthesis of PC creates an NPC-1 like mutation

An integral part of any pathway is the requirement for all necessary substrates. The compound R-Propranolol (Prop) has been shown to inhibit phosphatidic acid phosphohydrolase (PAP), an enzyme needed to convert phosphatidic acid (PA) into diacylglycerol (DAG) (74). DAG is used with CDP-choline to create PC (Figure 1.6) (59). By using Prop, we can therefore halt the CDP-choline pathway prior to PC formation.

CHO-7 cells are able to properly regulate their cholesterol machinery, as illustrated by their LDLR responses in Figure 3.5. Treating CHO-7 cells with LDL and Prop resulted in a distinctive lysosomal buildup of cholesterol, mirroring that observed in the SRD-2 and SRD-4 cells due to their cholesterol regulatory defects (Figure 3.9, A-C). Interestingly, the cholesterol buildup in these SRD cells also seemed to increase with the addition of Prop. By using the same lyso-PC treatment that was able to relieve the SRD cells of their lysosomal buildup, we saw clearance of a large majority of the Prop induced blockage in all cell lines (Figure 3.9, D-F). It would be of interest to monitor the cholesterol efflux from cells during these conditions, to determine if the excess cholesterol is being redistributed, effluxed or some combination of both of these mechanisms.

These results suggest that inhibiting the cells ability to synthesize PC can create a lysosomal cholesterol backup, which can in turn be alleviated with the addition of PC to the cell. This build up could be due to an imbalance in the PC to free cholesterol ratio within the cell caused by the lack of DAG. By providing the cell with the ability to make more PC, via lyso-PC, this would allow the cell to return the PC to free cholesterol ratio to a more normal level leading to the enhanced trafficking of cholesterol from within the lysosomes. It is interesting to note that upon the addition of Prop to the cells, the levels of NPC1 protein detectable by immunofluorescence increased in all cell types (Figure 3.12). This suggests that the cells are attempting to shuttle the cholesterol out of the lysosomal compartments but are unable to keep up with the demand due to the lack of PC. In all cases, flow cytometry was performed to ensure that the treatments did not prevent the uptake of LDL (Figure 3.13). Further research into the cholesterol blockage findings with the Prop compound need to be explored for better understanding of its effects. At this time we cannot rule out that Prop is having effects in addition to inhibiting PC synthesis. Future experiments will require specific knockdown of CCTα or other genetic methods to more specifically target PC metabolism.

4.4 Free Cholesterol Levels within ER are Responsible for Movement out of Lysosomes

It is known that from the lysosomes the LDL-derived cholesterol will eventually traffic to other organelle membranes, including the plasma membrane and ER. In the ER, free cholesterol will be esterified by ACAT; however, the exact mechanisms regulating this movement of cholesterol are unknown. Several models have been proposed to describe how cholesterol is distributed to the cell after its uptake into endocytic compartments. These

models encompass all possibilities, including that cholesterol concentration rapidly increasing in the plasma membrane after loading, and when a threshold is reached cholesterol is then allowed to traffic into the ER (11, 52). A second model suggests that LDL-derived cholesterol is shuttled directly to the ER, independent of the plasma membrane (95).

In keeping with the protective aspect of cholesterol sequestration, we believe that it is the levels of free cholesterol within the ER that is, in part, responsible for the movement of cholesterol out of the lysosomal compartments. Under normal circumstances, the plasma membrane is the major site of free cholesterol within the cell (62). The SRD cell lines have disrupted cholesterol regulatory machinery and are, thus, subject to lysosomal cholesterol loading of free cholesterol in the presence of LDL. SRD-4 cells do not contain functioning ACAT (70). This is not true of the SRD-2 line. To determine the effect of ACAT on the clearance of these loaded lysosomes we incubated all three cell lines with LDL and the ACAT inhibitor (ACATi) 58-035 for 20 hours. This incubation showed an up-regulation in the amount of lysosomal loading in the SRD-2 cells (Figure 3.14, panels F and G). The SRD-2 cells also showed a faster rate of clearance during washout of the inhibitor when compared to the SRD-4 cells. This observation can be attributed to the ability of the SRD-2 cells to create cholesteryl ester from the free cholesterol of the lysosomes. The SRD-4 cells inability to do this hindered the clearance rate. These findings suggest that it is the levels of free cholesterol within the ER, where the ACAT enzyme resides, (60) that contribute to the ability of the cell to clear cholesterol from blocked compartments. The lack of ACAT activity in the SRD-4 cells may contribute to their lysosomal blockage, thus highlighting the importance of free cholesterol levels within the ER. These levels may act as a central

regulator in the movement of cholesterol out of the lysosomes. By using a cell line with impaired ACAT function we have shown that limiting the cells ability to regulate free cholesterol within the ER has a negative effect on lysosomal trafficking. A more striking experiment would include an SRD-4 cell line with a stable transfection of an ACAT plasmid. This cell line would then be subject LDL loading. Hypothetically, this cell line would not exhibit the same degree of lysosomal loading that the SRD-4 cells show. The ACAT activity would allow levels of free cholesterol within the ER to drop, thereby allowing the lysosomes to undergo the necessary cholesterol egress. This remains a forerunner in future directions within the lab.

4.5 Conclusion

Our understanding of cholesterol metabolism is increasing daily; however, there are still large areas of research for which we have only begun to scratch the surface. This study aims to shed light on the ever elusive mechanisms of cholesterol metabolism. More specifically, this study aimed to determine the role that PC has in the egress of LDL-derived cholesterol from within the lysosomal compartments and the mechanisms surrounding the action of the ACAT enzyme. By employing sterol regulatory defective (SRD) CHO cells, we were able to manipulate known cholesterol pathways. Due to their defects, the SRD cells accumulate LDL-derived free cholesterol within their lysosomal compartments. This was shown to be relieved by either decreasing the degree to which the cell degrade PC or by giving the cells the ability to increase the cellular PC mass. In a contrasting experiment, we were able to create a lysosomal blockage with the compound R-Propranolol in the parental cell line, CHO-7, which harbors no known defects in cholesterol metabolism. R-Propranolol

works by blocking the synthesis of DAG, a substrate needed to synthesize PC. This block was also able to be relieved with the addition of exogenous lyso-PC to the cell. These studies suggest that the PC mass within the cell can contribute to the egress of cholesterol from the lysosomal compartments. This may be due to the delicate balance of the PC to free cholesterol ratio within the cell. By providing the cell with more PC, this would allow the cell to take up more cholesterol without cholesterol overloading and toxicity, due to a large imbalance in PC to free cholesterol. Due to the lack of active ACAT within the SRD-4 cell line, we were able to perform a simple ACAT study. We employed the use of the ACAT inhibitor 58-03 on all cell lines. It was shown that the SRD-2 cells, which have functional ACAT, were able to clear the lysosomal blockage in a more timely fashion than the SRD-4 cells. This implies that cholesterol trafficking in LDL loaded cells is dependent on ACAT activity and, more specifically, levels of free cholesterol within the ER. Taken together, these studies suggest that ratios of PC to free cholesterol in downstream organelles can affect the egress of cholesterol out of the lysosomal compartments in cholesterol loaded cells. Future studies will determine the effect of facilitated cholesterol movement on the SREBP machinery and the ability of the cells to sense the overall cholesterol content.

5 References

1. **Abi-Mosleh, L., R. E. Infante, A. Radhakrishnan, J. L. Goldstein, and M. S. Brown.** 2009. Cyclodextrin overcomes deficient lysosome-to-endoplasmic reticulum transport of cholesterol in Niemann-Pick type C cells. Proc. Natl. Acad. Sci. U. S. A. **106:**19316-19321.

2. **Baburina, I. and S. Jackowski.** 1999. Cellular responses to excess phospholipid. J. Biol. Chem. **274:**9400-9408.

3. **Balsinde, J. and E. A. Dennis.** 1997. Function and inhibition of intracellular calcium-independent phospholipase A2. J. Biol. Chem. **272:**16069-16072.

4. **Barbour, S. E., A. Kapur, and C. L. Deal.** 1999. Regulation of phosphatidylcholine homeostasis by calcium-independent phospholipase A2. Biochim. Biophys. Acta **1439:**77-88.

5. **Beaumont, J. L., L. A. Carlson, G. R. Cooper, Z. Fejfar, D. S. Fredrickson, and T. Strasser.** 1970. Classification of hyperlipidaemias and hyperlipoproteinaemias. Bull. World Health Organ. **43:**891-915.

6. **Beglova, N. and S. C. Blacklow.** 2005. The LDL receptor: how acid pulls the trigger. Trends Biochem. Sci. **30:**309-317.

7. **Bickel, P. E., J. T. Tansey, and M. A. Welte.** 2009. PAT proteins, an ancient family of lipid droplet proteins that regulate cellular lipid stores. Biochim. Biophys. Acta **1791:**419-440.

8. **Bloch, K.** 1965. The biological synthesis of cholesterol. Science **150:**19-28.

9. **Boadu, E., R. C. Nelson, and G. A. Francis.** 2012. ABCA1-dependent mobilization of lysosomal cholesterol requires functional Niemann-Pick C2 but not Niemann-Pick C1 protein. Biochim. Biophys. Acta **1821:**396-404.

10. **Boadu, E., H. Y. Choi, D. W. Lee, E. I. Waddington, T. Chan, B. Asztalos, J. E. Vance, A. Chan, G. Castro, and G. A. Francis.** 2006. Correction of apolipoprotein A-I-mediated lipid efflux and high density lipoprotein particle formation in human Niemann-Pick type C disease fibroblasts. J. Biol. Chem. **281:**37081-37090.

11. **Brasaemle, D. L. and A. D. Attie.** 1990. Rapid intracellular transport of LDL-derived cholesterol to the plasma membrane in cultured fibroblasts. J. Lipid Res. **31:**103-112.

12. **Brown, A. J., L. Sun, J. D. Feramisco, M. S. Brown, and J. L. Goldstein.** 2002. Cholesterol addition to ER membranes alters conformation of SCAP, the SREBP escort protein that regulates cholesterol metabolism. Mol. Cell **10:**237-245.

13. **Brown, M. S. and J. L. Goldstein.** 2009. Cholesterol feedback: from Schoenheimer's bottle to Scap's MELADL. J. Lipid Res. **50 Suppl:**S15-27.

14. **Brown, M. S. and J. L. Goldstein.** 1997. The SREBP pathway: regulation of cholesterol metabolism by proteolysis of a membrane-bound transcription factor. Cell **89:**331-340.

15. **Brown, M. S. and J. L. Goldstein.** 1986. A receptor-mediated pathway for cholesterol homeostasis. Science **232:**34-47.

16. **Brown, M. S. and J. L. Goldstein.** 1985. The LDL receptor and HMG-CoA reductase--two membrane molecules that regulate cholesterol homeostasis. Curr. Top. Cell. Regul. **26:**3-15.

17. **Brown, M. S. and J. L. Goldstein.** 1979. Receptor-mediated endocytosis: insights from the lipoprotein receptor system. Proc. Natl. Acad. Sci. U. S. A. **76:**3330-3337.

18. **Brown, M. S. and J. L. Goldstein.** 1974. Familial hypercholesterolemia: defective binding of lipoproteins to cultured fibroblasts associated with impaired regulation of 3-hydroxy-3-methylglutaryl coenzyme A reductase activity. Proc. Natl. Acad. Sci. U. S. A. **71:**788-792.

19. **Brown, W. V., R. I. Levy, and D. S. Fredrickson.** 1970. Further characterization of apolipoproteins from the human plasma very low density lipoproteins. J. Biol. Chem. **245:**6588-6594.

20. **Cao, G., J. L. Goldstein, and M. S. Brown.** 1996. Complementation of mutation in acyl-CoA:cholesterol acyltransferase (ACAT) fails to restore sterol regulation in ACAT-defective sterol-resistant hamster cells. J. Biol. Chem. **271:**14642-14648.

21. **Carstea, E. D., J. A. Morris, K. G. Coleman, S. K. Loftus, D. Zhang, C. Cummings, J. Gu, M. A. Rosenfeld, W. J. Pavan, D. B. Krizman, J. Nagle, M. H. Polymeropoulos, S. L. Sturley, Y. A. Ioannou, M. E. Higgins, M. Comly, A. Cooney, A. Brown, C. R. Kaneski, E. J. Blanchette-Mackie, N. K. Dwyer, E. B. Neufeld, T. Y. Chang, L. Liscum, J. F. Strauss 3rd, K. Ohno, M. Zeigler, R. Carmi, J. Sokol, D. Markie, R. R. O'Neill, O. P. van Diggelen, M. Elleder, M. C. Patterson, R. O. Brady, M. T. Vanier, P. G. Pentchev, and D. A. Tagle.** 1997. Niemann-Pick C1 disease gene: homology to mediators of cholesterol homeostasis. Science **277:**228-231.

22. **Cham, B. E.** 1978. Importance of apolipoproteins in lipid metabolism. Chem. Biol. Interact. **20:**263-277.

23. **Choi, H. Y., B. Karten, T. Chan, J. E. Vance, W. L. Greer, R. A. Heidenreich, W. S. Garver, and G. A. Francis.** 2003. Impaired ABCA1-dependent lipid efflux and hypoalphalipoproteinemia in human Niemann-Pick type C disease. J. Biol. Chem. **278:**32569-32577.

24. **Choudhury, A., D. K. Sharma, D. L. Marks, and R. E. Pagano.** 2004. Elevated endosomal cholesterol levels in Niemann-Pick cells inhibit rab4 and perturb membrane recycling. Mol. Biol. Cell **15:**4500-4511.

25. **Choudhury, A., M. Dominguez, V. Puri, D. K. Sharma, K. Narita, C. L. Wheatley, D. L. Marks, and R. E. Pagano.** 2002. Rab proteins mediate Golgi transport of caveola-internalized glycosphingolipids and correct lipid trafficking in Niemann-Pick C cells. J. Clin. Invest. **109:**1541-1550.

26. **Cornell, R. B. and H. Goldfine.** 1983. The coordination of sterol and phospholipid synthesis in cultured myogenic cells. Effect of cholesterol synthesis inhibition on the synthesis of phosphatidylcholine. Biochim. Biophys. Acta **750:**504-520.

27. **Cui, Z., M. Houweling, M. H. Chen, M. Record, H. Chap, D. E. Vance, and F. Terce.** 1996. A genetic defect in phosphatidylcholine biosynthesis triggers apoptosis in Chinese hamster ovary cells. J. Biol. Chem. **271:**14668-14671.

28. **Davies, J. P. and Y. A. Ioannou.** 2000. Topological analysis of Niemann-Pick C1 protein reveals that the membrane orientation of the putative sterol-sensing domain is identical to those of 3-hydroxy-3-methylglutaryl-CoA reductase and sterol regulatory element binding protein cleavage-activating protein. J. Biol. Chem. **275:**24367-24374.

29. **DeLong, C. J., Y. J. Shen, M. J. Thomas, and Z. Cui.** 1999. Molecular distinction of phosphatidylcholine synthesis between the CDP-choline pathway and phosphatidylethanolamine methylation pathway. J. Biol. Chem. **274:**29683-29688.

30. **Dorn, B. R., W. A. Dunn Jr, and A. Progulske-Fox.** 1999. Invasion of human coronary artery cells by periodontal pathogens. Infect. Immun. **67:**5792-5798.

31. **Du, H., M. Heur, D. P. Witte, D. Ameis, and G. A. Grabowski.** 2002. Lysosomal acid lipase deficiency: correction of lipid storage by adenovirus-mediated gene transfer in mice. Hum. Gene Ther. **13:**1361-1372.

32. **Esko, J. D., M. Nishijima, and C. R. Raetz.** 1982. Animal cells dependent on exogenous phosphatidylcholine for membrane biogenesis. Proc. Natl. Acad. Sci. U. S. A. **79:**1698-1702.

33. **Fernandez-Hernando, C., Y. Suarez, K. J. Rayner, and K. J. Moore.** 2011. MicroRNAs in lipid metabolism. Curr. Opin. Lipidol. **22:**86-92.

34. **Garver, W. S., D. Jelinek, G. A. Francis, and B. D. Murphy.** 2008. The Niemann-Pick C1 gene is downregulated by feedback inhibition of the SREBP pathway in human fibroblasts. J. Lipid Res. **49:**1090-1102.

35. **Garver, W. S., K. Krishnan, J. R. Gallagos, M. Michikawa, G. A. Francis, and R. A. Heidenreich.** 2002. Niemann-Pick C1 protein regulates cholesterol transport to the trans-Golgi network and plasma membrane caveolae. J. Lipid Res. **43:**579-589.

36. **Gevry, N., K. Schoonjans, F. Guay, and B. D. Murphy.** 2008. Cholesterol supply and SREBPs modulate transcription of the Niemann-Pick C-1 gene in steroidogenic tissues. J. Lipid Res. **49:**1024-1033.

37. **Gibellini, F. and T. K. Smith.** 2010. The Kennedy pathway--De novo synthesis of phosphatidylethanolamine and phosphatidylcholine. IUBMB Life **62:**414-428.

38. **Glomset, J. A.** 1968. The plasma lecithins:cholesterol acyltransferase reaction. J. Lipid Res. **9:**155-167.

39. **Goldman, S. D. and J. P. Krise.** 2010. Niemann-Pick C1 functions independently of Niemann-Pick C2 in the initial stage of retrograde transport of membrane-impermeable lysosomal cargo. J. Biol. Chem. **285:**4983-4994.

40. **Goldstein, J. L. and M. S. Brown.** 1985. The LDL receptor and the regulation of cellular cholesterol metabolism. J. Cell Sci. Suppl. **3:**131-137.

41. **Goldstein, J. L. and M. S. Brown.** 1973. Familial hypercholesterolemia: identification of a defect in the regulation of 3-hydroxy-3-methylglutaryl coenzyme A reductase activity associated with overproduction of cholesterol. Proc. Natl. Acad. Sci. U. S. A. **70:**2804-2808.

42. **Gong, Y., J. N. Lee, P. C. Lee, J. L. Goldstein, M. S. Brown, and J. Ye.** 2006. Sterol-regulated ubiquitination and degradation of Insig-1 creates a convergent mechanism for feedback control of cholesterol synthesis and uptake. Cell. Metab. **3:**15-24.

43. **Gorter, E. and F. Grendel.** 1925. On Bimolecular Layers of Lipoids on the Chromocytes of the Blood. J. Exp. Med. **41:**439-443.

44. **Gould, R. G., C. B. Taylor, J. S. Hagerman, I. Warner, And D. J. Campbell.** 1953. Cholesterol metabolism. I. Effect of dietary cholesterol on the synthesis of cholesterol in dog tissue in vitro. J. Biol. Chem. **201:**519-528.

45. **Greenspan, P., E. P. Mayer, and S. D. Fowler.** 1985. Nile red: a selective fluorescent stain for intracellular lipid droplets. J. Cell Biol. **100:**965-973.

45a. **Hara, S., S. Tsutomu, N. Takasu, And T. Mizui.** 1997. Lysophophatidylcholine promotes cholesterol efflux from mouse macrophage foam cells. Arterioscl Throm Vas. **17**: 1258-1266.

46. **Hermansson, M., K. Hokynar, and P. Somerharju.** 2011. Mechanisms of glycerophospholipid homeostasis in mammalian cells. Prog. Lipid Res. **50:**240-257.

47. **Hua, X., A. Nohturfft, J. L. Goldstein, and M. S. Brown.** 1996. Sterol resistance in CHO cells traced to point mutation in SREBP cleavage-activating protein. Cell **87:**415-426.

48. **Hua, X., C. Yokoyama, J. Wu, M. R. Briggs, M. S. Brown, J. L. Goldstein, and X. Wang.** 1993. SREBP-2, a second basic-helix-loop-helix-leucine zipper protein that stimulates transcription by binding to a sterol regulatory element. Proc. Natl. Acad. Sci. U. S. A. **90:**11603-11607.

49. **Infante, R. E., M. L. Wang, A. Radhakrishnan, H. J. Kwon, M. S. Brown, and J. L. Goldstein.** 2008. NPC2 facilitates bidirectional transfer of cholesterol between NPC1 and lipid bilayers, a step in cholesterol egress from lysosomes. Proc. Natl. Acad. Sci. U. S. A. **105:**15287-15292.

50. **Jacobs, R. L., Y. Zhao, D. P. Koonen, T. Sletten, B. Su, S. Lingrell, G. Cao, D. A. Peake, M. S. Kuo, S. D. Proctor, B. P. Kennedy, J. R. Dyck, and D. E. Vance.** 2010. Impaired de novo choline synthesis explains why phosphatidylethanolamine N-methyltransferase-deficient mice are protected from diet-induced obesity. J. Biol. Chem. **285:**22403-22413.

51. **Jelinek, D., S. M. Patrick, K. N. Kitt, T. Chan, G. A. Francis, and W. S. Garver.** 2009. Physiological and coordinate downregulation of the NPC1 and NPC2 genes are associated with the sequestration of LDL-derived cholesterol within endocytic compartments. J. Cell. Biochem. **108:**1102-1116.

52. **Johnson, W. J., G. K. Chacko, M. C. Phillips, and G. H. Rothblat.** 1990. The efflux of lysosomal cholesterol from cells. J. Biol. Chem. **265:**5546-5553.

53. **Jones, N. L., J. W. Reagan, and M. C. Willingham.** 2000. The pathogenesis of foam cell formation: modified LDL stimulates uptake of co-incubated LDL via macropinocytosis. Arterioscler. Thromb. Vasc. Biol. **20:**773-781.

54. **Kaptzan, T., S. A. West, E. L. Holicky, C. L. Wheatley, D. L. Marks, T. Wang, K. B. Peake, J. Vance, S. U. Walkley, and R. E. Pagano.** 2009. Development of a Rab9 transgenic mouse and its ability to increase the lifespan of a murine model of Niemann-Pick type C disease. Am. J. Pathol. **174:**14-20.

55. **Kent, C.** 1997. CTP:phosphocholine cytidylyltransferase. Biochim. Biophys. Acta **1348:**79-90.

56. **Kruth, H. S., M. E. Comly, J. D. Butler, M. T. Vanier, J. K. Fink, D. A. Wenger, S. Patel, and P. G. Pentchev.** 1986. Type C Niemann-Pick disease. Abnormal metabolism of low density lipoprotein in homozygous and heterozygous fibroblasts. J. Biol. Chem. **261:**16769-16774.

57. **Kwon, H. J., L. Abi-Mosleh, M. L. Wang, J. Deisenhofer, J. L. Goldstein, M. S. Brown, and R. E. Infante.** 2009. Structure of N-terminal domain of NPC1 reveals distinct subdomains for binding and transfer of cholesterol. Cell **137:**1213-1224.

58. **Lagace, T. A., M. K. Storey, and N. D. Ridgway.** 2000. Regulation of phosphatidylcholine metabolism in Chinese hamster ovary cells by the sterol regulatory element-binding protein (SREBP)/SREBP cleavage-activating protein pathway. J. Biol. Chem. **275:**14367-14374.

59. **Lim, P., R. Cornell, and D. E. Vance.** 1986. The supply of both CDP-choline and diacylglycerol can regulate the rate of phosphatidylcholine synthesis in HeLa cells. Biochem. Cell Biol. **64:**692-698.

60. **Lin, S., D. Cheng, M. S. Liu, J. Chen, and T. Y. Chang.** 1999. Human acyl-CoA:cholesterol acyltransferase-1 in the endoplasmic reticulum contains seven transmembrane domains. J. Biol. Chem. **274:**23276-23285.

61. **Linton, M. F. and S. Fazio.** 2003. Macrophages, inflammation, and atherosclerosis. Int. J. Obes. Relat. Metab. Disord. **27 Suppl 3:**S35-40.

62. **Liscum, L. and J. R. Faust.** 1994. Compartmentation of cholesterol within the cell. Curr. Opin. Lipidol. **5:**221-226.

63. **Liscum, L. and J. R. Faust.** 1989. The intracellular transport of low density lipoprotein-derived cholesterol is inhibited in Chinese hamster ovary cells cultured with 3-beta-[2-(diethylamino)ethoxy]androst-5-en-17-one. J. Biol. Chem. **264:**11796-11806.

64. **Liscum, L. and J. R. Faust.** 1987. Low density lipoprotein (LDL)-mediated suppression of cholesterol synthesis and LDL uptake is defective in Niemann-Pick type C fibroblasts. J. Biol. Chem. **262:**17002-17008.

65. **Listenberger, L. L. and D. A. Brown.** 2007. Fluorescent detection of lipid droplets and associated proteins. Curr. Protoc. Cell. Biol. **Chapter 24:**Unit 24.2.

66. **Liu, B., S. D. Turley, D. K. Burns, A. M. Miller, J. J. Repa, and J. M. Dietschy.** 2009. Reversal of defective lysosomal transport in NPC disease ameliorates liver dysfunction and neurodegeneration in the npc1-/- mouse. Proc. Natl. Acad. Sci. U. S. A. **106:**2377-2382.

67. **Marcel, Y. L., M. Ouimet, and M. D. Wang.** 2008. Regulation of cholesterol efflux from macrophages. Curr. Opin. Lipidol. **19:**455-461.

68. **McCauliff, L. A., Z. Xu, and J. Storch.** 2011. Sterol transfer between cyclodextrin and membranes: similar but not identical mechanism to NPC2-mediated cholesterol transfer. Biochemistry **50:**7341-7349.

69. **McIntosh, T. J.** 1996. Hydration properties of lamellar and non-lamellar phases of phosphatidylcholine and phosphatidylethanolamine. Chem. Phys. Lipids **81:**117-131.

70. **Metherall, J. E., N. D. Ridgway, P. A. Dawson, J. L. Goldstein, and M. S. Brown.** 1991. A 25-hydroxycholesterol-resistant cell line deficient in acyl-CoA: cholesterol acyltransferase. J. Biol. Chem. **266:**12734-12740.

71. **Morris, M. D., C. Bhuvaneswaran, H. Shio, and S. Fowler.** 1982. Lysosome lipid storage disorder in NCTR-BALB/c mice. I. Description of the disease and genetics. Am. J. Pathol. **108:**140-149.

72. **Naureckiene, S., D. E. Sleat, H. Lackland, A. Fensom, M. T. Vanier, R. Wattiaux, M. Jadot, and P. Lobel.** 2000. Identification of HE1 as the second gene of Niemann-Pick C disease. Science **290:**2298-2301.

73. **Nohturfft, A., X. Hua, M. S. Brown, and J. L. Goldstein.** 1996. Recurrent G-to-A substitution in a single codon of SREBP cleavage-activating protein causes sterol resistance in three mutant Chinese hamster ovary cell lines. Proc. Natl. Acad. Sci. U. S. A. **93:**13709-13714.

74. **Pappu, A. S. and G. Hauser.** 1983. Propranolol-induced inhibition of rat brain cytoplasmic phosphatidate phosphohydrolase. Neurochem. Res. **8:**1565-1575.

75. **Peake, K. B. and J. E. Vance.** 2012. Normalization of cholesterol homeostasis by 2-hydroxypropyl-beta-cyclodextrin in neurons and glia from Niemann-Pick C1 (NPC1)-deficient mice. J. Biol. Chem. **287:**9290-9298.

76. **Perez-Chacon, G., A. M. Astudillo, V. Ruiperez, M. A. Balboa, and J. Balsinde.** 2010. Signaling role for lysophosphatidylcholine acyltransferase 3 in receptor-regulated arachidonic acid reacylation reactions in human monocytes. J. Immunol. **184:**1071-1078.

77. **Peterson, G. L.** 1977. A simplification of the protein assay method of Lowry et al. which is more generally applicable. Anal. Biochem. **83:**346-356.

78. **Radhakrishnan, A., Y. Ikeda, H. J. Kwon, M. S. Brown, and J. L. Goldstein.** 2007. Sterol-regulated transport of SREBPs from endoplasmic reticulum to Golgi: oxysterols block transport by binding to Insig. Proc. Natl. Acad. Sci. U. S. A. **104:**6511-6518.

79. **Ridgway, N. D., D. M. Byers, H. W. Cook, and M. K. Storey.** 1999. Integration of phospholipid and sterol metabolism in mammalian cells. Prog. Lipid Res. **38:**337-360.

80. **Robichaud, J. C., J. N. van der Veen, Z. Yao, B. Trigatti, and D. E. Vance.** 2009. Hepatic uptake and metabolism of phosphatidylcholine associated with high density lipoproteins. Biochim. Biophys. Acta **1790:**538-551.

81. **Rosenbaum, A. I., G. Zhang, J. D. Warren, and F. R. Maxfield.** 2010. Endocytosis of beta-cyclodextrins is responsible for cholesterol reduction in Niemann-Pick type C mutant cells. Proc. Natl. Acad. Sci. U. S. A. **107:**5477-5482.

82. **Ross, A. C., K. J. Go, J. G. Heider, and G. H. Rothblat.** 1984. Selective inhibition of acyl coenzyme A:cholesterol acyltransferase by compound 58-035. J. Biol. Chem. **259:**815-819.

83. **Sato, R., J. Inoue, Y. Kawabe, T. Kodama, T. Takano, and M. Maeda.** 1996. Sterol-dependent transcriptional regulation of sterol regulatory element-binding protein-2. J. Biol. Chem. **271:**26461-26464.

84. **Seashols, S. J., A. del Castillo Olivares, G. Gil, and S. E. Barbour.** 2004. Regulation of group VIA phospholipase A2 expression by sterol availability. Biochim. Biophys. Acta **1684:**29-37.

85. **Shimomura, I., H. Shimano, J. D. Horton, J. L. Goldstein, and M. S. Brown.** 1997. Differential expression of exons 1a and 1c in mRNAs for sterol regulatory element binding protein-1 in human and mouse organs and cultured cells. J. Clin. Invest. **99:**838-845.

86. **Shiratori, Y., A. K. Okwu, and I. Tabas.** 1994. Free cholesterol loading of macrophages stimulates phosphatidylcholine biosynthesis and up-regulation of CTP: phosphocholine cytidylyltransferase. J. Biol. Chem. **269:**11337-11348.

87. **Smith, J. R., T. F. Osborne, J. L. Goldstein, and M. S. Brown.** 1990. Identification of nucleotides responsible for enhancer activity of sterol regulatory element in low density lipoprotein receptor gene. J. Biol. Chem. **265:**2306-2310.

88. **Subczynski, W. K. and A. Wisniewska.** 2000. Physical properties of lipid bilayer membranes: relevance to membrane biological functions. Acta Biochim. Pol. **47:**613-625.

89. **Sun, L. P., J. Seemann, J. L. Goldstein, and M. S. Brown.** 2007. Sterol-regulated transport of SREBPs from endoplasmic reticulum to Golgi: Insig renders sorting signal in Scap inaccessible to COPII proteins. Proc. Natl. Acad. Sci. U. S. A. **104:**6519-6526.

90. **Sun, L. P., L. Li, J. L. Goldstein, and M. S. Brown.** 2005. Insig required for sterol-mediated inhibition of Scap/SREBP binding to COPII proteins in vitro. J. Biol. Chem. **280:**26483-26490.

91. **Tabas, I.** 2002. Consequences of cellular cholesterol accumulation: basic concepts and physiological implications. J. Clin. Invest. **110:**905-911.

92. **Tabas, I.** 1997. Phospholipid metabolism in cholesterol-loaded macrophages. Curr. Opin. Lipidol. **8:**263-267.

93. **Tabas, I., S. Marathe, G. A. Keesler, N. Beatini, and Y. Shiratori.** 1996. Evidence that the initial up-regulation of phosphatidylcholine biosynthesis in free cholesterol-loaded macrophages is an adaptive response that prevents cholesterol-induced cellular necrosis. Proposed role of an eventual failure of this response in foam cell necrosis in advanced atherosclerosis. J. Biol. Chem. **271:**22773-22781.

94. **Ullery-Ricewick, J. C., B. E. Cox, E. E. Griffin, and W. G. Jerome.** 2009. Triglyceride alters lysosomal cholesterol ester metabolism in cholesteryl ester-laden macrophage foam cells. J. Lipid Res. **50:**2014-2026.

95. **Underwood, K. W., N. L. Jacobs, A. Howley, and L. Liscum.** 1998. Evidence for a cholesterol transport pathway from lysosomes to endoplasmic reticulum that is independent of the plasma membrane. J. Biol. Chem. **273:**4266-4274.

96. **Vance, D. E., E. M. Trip, and H. B. Paddon.** 1980. Poliovirus increases phosphatidylcholine biosynthesis in HeLa cells by stimulation of the rate-limiting reaction catalyzed by CTP: phosphocholine cytidylyltransferase. J. Biol. Chem. **255:**1064-1069.

97. **Yan, D., M. Lehto, L. Rasilainen, J. Metso, C. Ehnholm, S. Yla-Herttuala, M. Jauhiainen, and V. M. Olkkonen.** 2007. Oxysterol binding protein induces upregulation of SREBP-1c and enhances hepatic lipogenesis. Arterioscler. Thromb. Vasc. Biol. **27:**1108-1114.

98. **Yang, J., M. S. Brown, Y. K. Ho, and J. L. Goldstein.** 1995. Three different rearrangements in a single intron truncate sterol regulatory element binding protein-2 and produce sterol-resistant phenotype in three cell lines. Role of introns in protein evolution. J. Biol. Chem. **270:**12152-12161.

99. **Yang, J., R. Sato, J. L. Goldstein, and M. S. Brown.** 1994. Sterol-resistant transcription in CHO cells caused by gene rearrangement that truncates SREBP-2. Genes Dev. **8:**1910-1919.

100. **Yang, T., P. J. Espenshade, M. E. Wright, D. Yabe, Y. Gong, R. Aebersold, J. L. Goldstein, and M. S. Brown.** 2002. Crucial step in cholesterol homeostasis: sterols promote binding of SCAP to INSIG-1, a membrane protein that facilitates retention of SREBPs in ER. Cell **110:**489-500.

101. **Zelcer, N., C. Hong, R. Boyadjian, and P. Tontonoz.** 2009. LXR regulates cholesterol uptake through Idol-dependent ubiquitination of the LDL receptor. Science **325:**100-104.

102. **Zhang, D., W. Tang, P. M. Yao, C. Yang, B. Xie, S. Jackowski, and I. Tabas.** 2000. Macrophages deficient in CTP:Phosphocholine cytidylyltransferase-alpha are viable under normal culture conditions but are highly susceptible to free cholesterol-induced death. Molecular genetic evidence that the induction of phosphatidylcholine biosynthesis in free cholesterol-loaded macrophages is an adaptive response. J. Biol. Chem. **275:**35368-35376.

Curriculum Vitae

Education

May 2010-June 2012	M.Sc. in Biochemistry University of Ottawa Department of Biochemistry, Microbiology and Immunology "Phosphatidylcholine Metabolism and ACAT Affect the Trafficking Of LDL-derived Free Cholesterol in Cholesterol-loaded CHO Cells"
Sept 2005- April 2009	Honours B.Sc. with Specialization in Biochemistry University of Ottawa Department of Biochemistry, Microbiology and Immunology

Awards

Sept 2005-May 2006	Admissions Scholarship, University of Ottawa

Presentations

I presented all listed below with the exception of number 10:

1. Landry, C., and Lagace, T., "Phosphatidylcholine metabolism and ACAT affects trafficking of LDL-derived free cholesterol in choelsterol laoded CHO cells." **Poster.** University of Ottawa Heart Institute, Research Day, Ottawa, Ontario, May 2012.
2. Landry, C., and Lagace, T., "Phosphatidylcholine metabolism and ACAT affects trafficking of LDL-derived free cholesterol in choelsterol laoded CHO cells." **Poster.** Canadian Lipoprotein Conference, Halifax, Nova Scotia, November, 2011.
3. Landry, C., and Lagace, T., "Phosphatidylcholine affects trafficking of LDL-derived free cholesterol in choelsterol laoded CHO cells." **Poster.** University of Ottawa Departmental Biochemistry, Microbiology and Immunology Graduate Student Poster Day, Ottawa, Ontario, October, 2011.
4. Landry, C., and Lagace, T., "Phosphatidylcholine affects trafficking of LDL-derived free cholesterol in choelsterol laoded CHO cells." **Oral talk.** University of Ottawa Heart Institute Research Day, Ottawa, Ontario, May, 2011.
5. Landry, C., and Lagace, T., "Phosphatidylcholine affects trafficking of LDL-derived free cholesterol in choelsterol laoded CHO cells." **Poster.** Cardiovascular Symposium, Ottawa, Ontario, May, 2011.
6. Landry, C., and Lagace, T., "Phosphatidylcholine affects trafficking of LDL-derived free cholesterol in choelsterol laoded CHO cells." **Poster.** Department of Medicine and Labaratory Pathology Poster Day, Ottawa, Ontario, April, 2011.
7. Landry, C., and Lagace, T., "Phosphatidylcholine affects trafficking of LDL-derived free cholesterol in choelsterol laoded CHO cells." **Poster.** Canadian Lipoprotein Conference, Niagra-on-the-Lake, Ontario, October, 2010.
8. Landry, C., and Lagace, T., "Phosphatidylcholine affects trafficking of LDL-derived free

cholesterol in choelsterol laoded CHO cells." **Poster.** University of Ottawa Heart Institute Research Day, Ottawa, Ontario, May, 2010.

9. Landry, C., Gage, J., Whitman, SC. "Examining the Mouse Strain Specific Cytokine Profiles Originating from Macrophages Challenged with the Oral Pathogen *P gingivalis*." **Oral talk**. University of Ottawa Undergraduate Seminars, Ottawa, Ontario, March, 2009.

10. Gage, J., Landry, C., Baskaran, P. Whitman, SC. "Cytokine Profiling of Macrophages and Foam Cells Exposed to Live *Porphyromonas gingivalis*." **Poster**. ATVB, Washington, USA, April, 2009.